Chapter 2

Waves in Isotropic Media

2.1 INTRODUCTION

In this chapter we describe the various types of waves that can exist in isotropic media. In Sec. 2.2 we introduce the commonly used notation for the elastic constants in isotropic media and then derive the wave equations for propagation of longitudinal and shear waves. These will be stated in terms of potential functions, in a similar manner as in electromagnetic (EM) theory. We also discuss the basic concepts of reflection and refraction at the boundary between two media, stressing their importance to various types of mode conversion schemes.

Section 2.3 carries these ideas further by giving a short description of some of the various kinds of waveguide modes that can exist in bounded media. We then consider the important topic of surface acoustic waves and give the basic derivation for Rayleigh waves in an isotropic medium.

We describe the properties of the interdigital transducer in Sec. 2.4, and the delta function model is given, together with the network theory for determining its impedance.

In Sec. 2.5, we derive a perturbation theory or *normal-mode theory* that is used to calculate excitation and perturbation of waves in a waveguide. First we show how this theory may be applied to various problems; then we use it to determine the impedance of an interdigital transducer. Next we introduce the concept of *leaky waves* and determine the attenuation of leaky Rayleigh waves propagating on a surface loaded by water. Finally, we employ the leaky wave theory to derive the properties of the wedge transducer.

2.2 BASIC THEORY FOR WAVES IN ISOTROPIC MEDIA

2.2.1 Mathematical Formalism for Waves in Isotropic Media

Here we show how the tensor formalism for acoustic waves given in Sec. 1.5 and Appendix A can be simplified for isotropic media [1–6]. We use the condition that only two independent elastic constants can exist in an isotropic medium; these determine the ratio between the shear wave velocity and the longitudinal wave velocity. As we show, this ratio must be between 0 and 0.707; for many solids it is approximately 0.5. Because liquids cannot support shear stresses, their shear wave velocities must always be zero. In liquids, the stress components in all directions are equal in magnitude, which means that the stress can be expressed in terms of pressure, a scalar quantity. Materials such as polyethylene or rubber have very small ratios of shear to longitudinal wave velocity and thus behave like viscous liquids. We also define *Poisson's ratio* [2], a parameter used frequently in solid mechanics.

We shall find it convenient to derive the reciprocal relations to the elastic constitutive equations so that we can determine strain in terms of stress. The expressions obtained will be stated in terms of Poisson's ratio and an elasticity parameter known as *Young's modulus*. Such relations are particularly convenient for dealing with wave propagation along thin rods for which the applied stresses normal to the surface of the rod are zero. As the frequency is reduced to zero and the wavelength becomes much larger than the cross-sectional dimensions of the rod, these relations reduce to simple forms used in statics.

Lamé constants. We have shown in Appendix A that, due to symmetry, the number of independent elastic constants in an isotropic medium reduces to two. In the literature, these two independent constants are called the Lamé constants, λ and μ [1–6]. These parameters are useful for determining the total stored energy of the system [see Eq. (2.2.11)] and are related to the elastic constants already defined, as follows:

$$c_{11} = c_{22} = c_{33} = \lambda + 2\mu \tag{2.2.1}$$

$$c_{12} = c_{13} = c_{23} = c_{21} = c_{31} = c_{32} = \lambda \tag{2.2.2}$$

and

$$c_{44} = c_{55} = c_{66} = \mu = \frac{c_{11} - c_{12}}{2} \tag{2.2.3}$$

All the other off-diagonal terms are zero. The parameter μ is known as the *shear modulus*, or the modulus of rigidity.

Dilation and Hooke's law. The relation between stress and strain can be written in several equivalent forms. One way to write it is in the reduced tensor notation introduced in Sec. 1.5 and Appendix A:

$$T_I = c_{IJ} S_J \tag{2.2.4}$$

A second convenient way to state this relation is in a dyadic form:

$$\mathbf{T} = \mathbf{c} : \mathbf{S} \tag{2.2.5}$$

For isotropic materials, the relation between longitudinal stress and strain is

$$T_1 = c_{11}S_1 + c_{12}S_2 + c_{13}S_3$$

$$= \lambda(S_1 + S_2 + S_3) + 2\mu S_1 = \lambda\Delta + 2\mu S_1 \tag{2.2.6}$$

or, in general,

$$T_I = \lambda\Delta + 2\mu S_I \qquad (I = 1, 2, 3) \tag{2.2.7}$$

where we have defined Δ, the *dilation*, as

$$\Delta = S_1 + S_2 + S_3 \tag{2.2.8}$$

or the fractional change in volume of the material [see Eq. (A.16)], that is, the sum of the fractional extensions of a cube along the x, y, and z axes.

The similar shear relations are

$$\begin{aligned} T_4 &= \mu S_4 \\ T_5 &= \mu S_5 \\ T_6 &= \mu S_6 \end{aligned} \tag{2.2.9}$$

Energy. The stored elastic energy W_c is defined as

$$W_c = \tfrac{1}{2}T_I S_I = \tfrac{1}{2}\mathbf{T} : \mathbf{S} \tag{2.2.10}$$

For an isotropic material this relationship may be written in the following form:

$$W_S = \tfrac{1}{2}\lambda\Delta^2 + \mu(S_1^2 + S_2^2 + S_3^2) + \frac{\mu}{2}(S_4^2 + S_5^2 + S_6^2) \tag{2.2.11}$$

Ideal fluid. An ideal fluid cannot support shear stresses. Hence $\mu = 0$, $c_{11} = c_{12} = \lambda$, $c_{44} = 0$, and, from Eq. (2.2.7), $T_1 = T_2 = T_3 = \lambda\Delta$. Thus we can define the pressure p in a fluid in terms of the stress within a small volume, as follows:

$$p = -T_1 = -T_2 = -T_3 = -\kappa\Delta \tag{2.2.12}$$

The parameter $\kappa = T/(S_1+S_2+S_3)$ is called *the bulk elastic modulus*. More generally, in a solid, when μ is finite, Eq. (2.2.7) shows that we can still write $p = -\kappa\Delta$, provided that we now define p in terms of the average stress as

$$p = \frac{-(T_1 + T_2 + T_3)}{3} \tag{2.2.13}$$

and put

$$\kappa = \lambda + 2\mu/3 \tag{2.2.14}$$

A perfectly incompressible material would have $\kappa = \infty$, whereas an easily compressible medium such as air has a very small κ compared to that of water [κ(water)/κ(air) = 19,000]. This relation is important when considering the propagation of waves through water containing air bubbles.

Young's modulus and the extensional wave velocity. Certain other notations are useful when dealing with stress in a thin rod. It is a simple matter to express the strain in terms of the stress. Equation (2.2.7) implies that

$$S_1 = \frac{\lambda + \mu}{\mu(3\lambda + 2\mu)} T_1 - \frac{\lambda}{2\mu(3\lambda + 2\mu)}(T_2 + T_3) \tag{2.2.15}$$

with symmetric expressions for S_2 and S_3.

Consider a thin rod stressed in the z direction so that the only finite component of stress is T_3. In this case the rod may bulge in the x and y directions so that S_1 and S_2 are finite. Putting $T_1 = T_2 = 0$, we find that

$$S_3 = \frac{T_3}{E} \tag{2.2.16}$$

where

$$E = \frac{1}{s_{11}} = \frac{\mu(3\lambda + 2\mu)}{\lambda + \mu} = c_{11} - \frac{2c_{12}^2}{c_{11} + c_{12}} \tag{2.2.17}$$

The parameter E is called *Young's modulus*; it is the elastic constant normally measured when a rod is stretched in a testing machine. The parameter s_{11} is defined in Sec. 1.5 and Appendix A. The longitudinal wave that propagates along a thin rod is called an *extensional wave*. It follows from Eq. (2.2.17) and the one-dimensional wave equation (1.1.11) that we can find the velocity of this wave by replacing c with E. The extensional wave velocity is therefore

$$V_e = \sqrt{\frac{E}{\rho_{m0}}} \tag{2.2.18}$$

Equations (2.2.17) and (2.2.18) imply that the extensional wave velocity V_e is always less than the longitudinal velocity V_l.

Poisson's ratio. Putting $T_1 = T_2 = 0$ in Eq. (2.2.15) and using Eqs. (2.2.16) and (2.2.17), we find that

$$S_1 = -\sigma S_3 \tag{2.2.19}$$

where the parameter σ is called *Poisson's ratio*, defined as

$$\sigma = \frac{\lambda}{2(\lambda + \mu)} = \frac{c_{12}}{c_{11} + c_{12}} = -\frac{s_{12}}{s_{11}} \tag{2.2.20}$$

Poisson's ratio is the ratio of the transverse compression to the longitudinal expansion of a thin rod to which a static longitudinal axial stress is applied. For a liquid, Poisson's ratio is 0.5; for a solid, it must be between 0 and 0.5. For

materials with a small modulus of rigidity, such as polyethylene or rubber, it is close to 0.5 ($\sigma = 0.46$ for polyethylene). For most metals it is of the order of 0.3; for beryllium, however, it is 0.05. For a perfect fluid, $\mu = 0$, $E = 0$, and $\sigma = 0.5$. Thus, if we ignore surface tension which may make T_1 and T_2 finite, a stream of liquid cannot support an extensional wave, so that $V_e = 0$. In seismic work, for reasons of mathematical convenience, it is sometimes assumed that $\lambda = \mu$. In this case, $E = 5/2\lambda$ and $\sigma = \frac{1}{4}$ with $\kappa = 5\lambda/3$; this value of σ is typical for ceramic materials and many types of rock.

It also follows from these relations that, in general,

$$S_1 = \frac{T_1}{E} - \frac{\sigma}{E}(T_2 + T_3) \tag{2.2.21}$$

with symmetric expressions for S_2 and S_3, and that

$$S_4 = \frac{2(1 + \sigma)}{E} T_4 = \frac{T_4}{\mu} \tag{2.2.22}$$

with similar expressions for S_5 and S_6. In mechanics texts, the constitutive relations are usually expressed in these forms because they are convenient to use for statics when there is no longitudinal stress variation over the cross section of a rod.

Suppose that we consider a thin rod of rubber or a thin stream of liquid, each aligned in the z direction. As the stresses T_1 and T_2 normal to the axis are zero, and as $\sigma = 0.5$, then $S_1 = S_2 = -S_3/2$. Thus the material expands in the transverse direction by half the amount it is compressed in the longitudinal direction. This is just what we would expect from conservation of mass, for when there is no restoring force on the outside of the rod, the volume of the material cannot change.

Shear, longitudinal, extensional, and strip guide wave velocities. The shear wave velocity V_s determined from the effective elastic constant for shear waves, $c_{44} = E$, is defined as $V_s = \sqrt{c_{44}/\rho_{m0}}$. The ratio of the shear wave velocity to the longitudinal wave velocity V_l is defined as

$$\frac{V_s}{V_l} = \sqrt{\frac{c_{44}}{c_{11}}} = \sqrt{\frac{\mu}{\lambda + 2\mu}} = \sqrt{\frac{0.5 - \sigma}{1 - \sigma}} \tag{2.2.23}$$

Similarly, the ratios of the extensional wave velocity V_e to the longitudinal and shear wave velocities are

$$\frac{V_e}{V_l} = \sqrt{\frac{E}{c_{11}}} = \sqrt{\frac{(1 + \sigma)(1 - 2\sigma)}{1 - \sigma}} \tag{2.2.24}$$

and

$$\frac{V_s}{V_e} = \sqrt{\frac{\mu}{E}} = \sqrt{\frac{1}{2(1 + \sigma)}} \tag{2.2.25}$$

respectively.

Finally, we give the results for an extensional wave propagating along a strip that is infinitesimally thin in the y direction and infinitely wide in the x direction. We call this wave a *strip guide mode*; for it, we assume that $T_2 = 0$ and $S_1 = 0$. We shall call its velocity V_L; the ratio of this velocity to the longitudinal wave velocity V_l is

$$\frac{V_L}{V_l} = \sqrt{1 - \left(\frac{c_{12}}{c_{11}}\right)^2} = \sqrt{\frac{1 - 2\sigma}{(1 - \sigma)^2}} \tag{2.2.26}$$

Plots of the values of V_s/V_l, V_e/V_l, V_s/V_e, and V_L/V_l as functions of Poisson's ratio are given in Fig. 2.2.1. For $\sigma = 0$, $V_s/V_l = 0.707$. As might be expected, rubber-like materials such as polyethylene ($\sigma = 0.46$) tend to have relatively large values of Poisson's ratio; because they behave somewhat like liquids, they have a small ratio of V_s/V_l. Harder materials such as ceramics and glasses tend to have smaller values of σ, and hence a larger ratio of V_s/V_l. Most metals have Poisson's ratios of the order of 0.3, with $V_s/V_l \sim 0.6$ and $V_e/V_l \sim 0.9$. Note that V_e/V_l, V_L/V_l, and V_s/V_l decrease monotonically with σ.

2.2.2 Equations of Motion for Solids and Fluids

It is shown in Sec. 1.5 and Appendix A that the force in the x direction on a cube of volume $dx\,dy\,dz$ due to a stress $T_1 = T_{xx}$ is $(\partial T_1/\partial x)\,dx\,dy\,dz$, or $\partial T_1/\partial x$ per unit volume. This is illustrated in Fig. 2.2.2(a). Similarly, as illustrated in Fig. 2.2.2(b), the force in the x direction on a cube of volume $dx\,dy\,dz$ due to a shear stress $T_6 = T_{xy}$ is $(\partial T_6/\partial y)\,dx\,dy\,dz$, or $\partial T_6/\partial y$ per unit volume [7]. A similar relation can be obtained for the force due to a shear stress about the y axis (a shear stress in the xz direction). Thus, as discussed more fully in Sec. 1.5 and

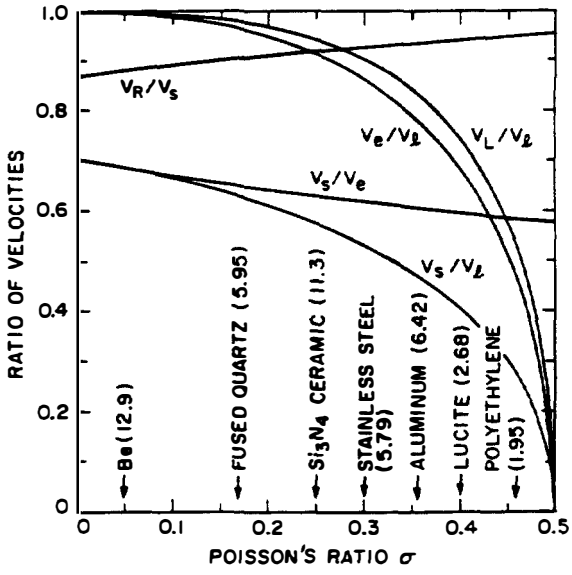

Figure 2.2.1 Relationships of velocity ratios to Poisson's ratio. The longitudinal wave velocities in km/s are given in brackets for various materials. V_l, Longitudinal wave velocity; V_e, extensional wave velocity; V_s, shear wave velocity; V_R, Rayleigh wave velocity; V_L, strip guide mode velocity.

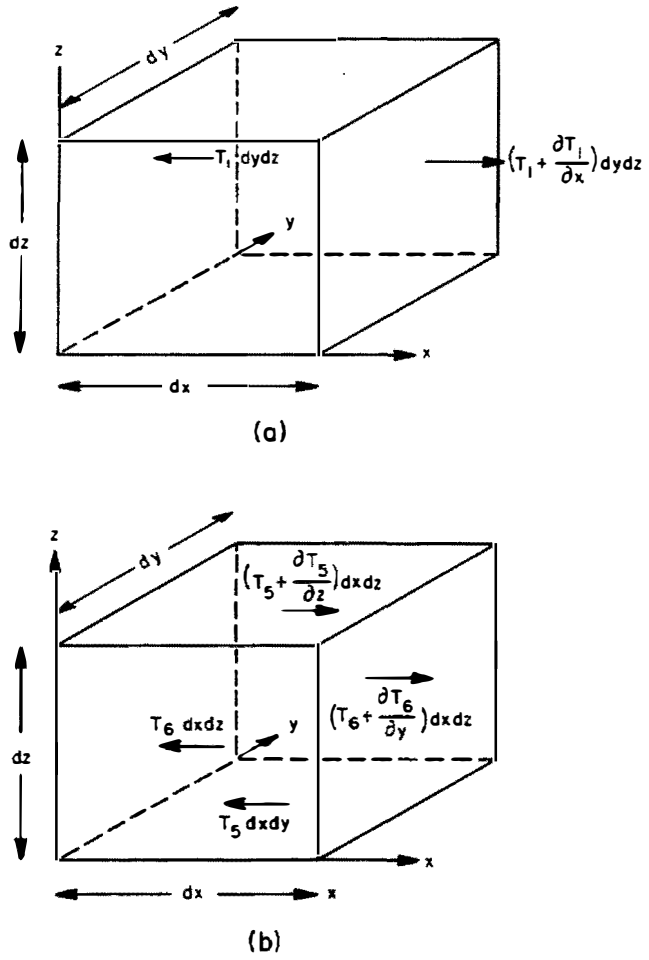

Figure 2.2.2 Stresses applied to a cube with sides dx, dy, and dz. (a) Longitudinal stress T_1; (b) shear stresses $T_5 = T_{xz}$ and $T_6 = T_{xy}$. The longitudinal stress applies forces to the faces x and $x + dx$ of the cube, while the shear stresses T_5 and T_6 apply forces to the faces z and $z + dz$, and y and $y + dy$, respectively.

Appendix A, after adding all the force terms, the equation of motion in the x direction is

$$\rho_{m0}\frac{\partial^2 u_x}{\partial t^2} = \frac{\partial T_1}{\partial x} + \frac{\partial T_6}{\partial y} + \frac{\partial T_5}{\partial z} \tag{2.2.27}$$

In full tensor notation, Eq. (2.2.27) may be written in the form

$$\rho_{m0}\frac{\partial^2 u_x}{\partial t^2} = \frac{\partial T_{xx}}{\partial x} + \frac{\partial T_{xy}}{\partial y} + \frac{\partial T_{xz}}{\partial z} \tag{2.2.28}$$

Similar relations for the equations of motion in the y and z directions can be obtained.

Following Auld [4], it is often convenient to use the symbolic notation, which is discussed more fully in Appendix A, and write

$$\nabla \cdot \mathbf{T} = \rho_{m0}\frac{\partial^2 \mathbf{u}}{\partial t^2} \tag{2.2.29}$$

Gauss's divergence theorem can often be used on this divergence term and physically meaningful formulas for surface stress can easily be derived from it.

In the full tensor notation, Eq. (2.2.29) is equivalent to

$$\frac{\partial T_{ij}}{\partial x_j} = \rho_{m0} \frac{\partial^2 u_i}{\partial t^2} \tag{2.2.30}$$

2.2.3 Wave Equation in an Isotropic Medium

We can substitute Eq. (2.2.6) into Eq. (2.2.29) or Eq. (2.2.30) to obtain an equation that relates the displacement in the x direction and the strain, as follows:

$$\rho_{m0} \frac{\partial^2 u_x}{\partial t^2} = \frac{\partial}{\partial x}(\lambda\Delta + 2\mu S_1) + \mu\left(\frac{\partial S_6}{\partial y} + \frac{\partial S_5}{\partial z}\right) \tag{2.2.31}$$

Similar expressions hold for $\partial^2 u_y/\partial t^2$ and $\partial^2 u_z/\partial t^2$. Note that the dilation Δ of the material, or the relative volume expansion, is defined as

$$\Delta = S_1 + S_2 + S_3 = \nabla \cdot \mathbf{u} \tag{2.2.32}$$

To obtain the wave equation for the displacement, we must use an additional relation between strain and displacement. As far as the longitudinal components of strain are concerned, this relation is the same as that derived in Eq. (1.1.2):

$$S_1 = \frac{\partial u_x}{\partial x} \tag{2.2.33}$$

Similar expressions exist for the other longitudinal components of strain.

To determine the shear strain component in the y-z plane, we must take account of the displacements in both the y and z directions. Generalizing the one-dimensional formulation in Sec. 1.1, we write

$$S_4 = \frac{\partial u_z}{\partial y} + \frac{\partial u_y}{\partial z} \tag{2.2.34}$$

with similar expressions for the other shear components of strain. These relations are derived in more detail in Appendix A. Following Auld [4], we can summarize them, with the symbolic notation defined in Appendix A, as

$$\mathbf{S} \approx \nabla_s \mathbf{u} \tag{2.2.35}$$

where $\nabla_s \mathbf{u}$ denotes the symmetric part of the dyadic $\nabla \mathbf{u}$. Alternatively, using the full tensor notation, we can write

$$S_{ij} = \frac{1}{2}\left(\frac{\partial u_i}{\partial x_j} + \frac{\partial u_j}{\partial x_i}\right) \tag{2.2.36}$$

Note the $\frac{1}{2}$ used in the definition of S_{ij} (see Sec. 1.5, Table 1.5.1, and Appendix A). By substituting for S_5 and S_6 from Eq. (2.2.35) or Eq. (2.2.36) into Eq. (2.2.31), we obtain (after some algebra) the relatively simple relation

$$\rho_{m0} \frac{\partial^2 \mathbf{u}}{\partial t^2} = (\lambda + 2\mu)\, \nabla(\nabla \cdot \mathbf{u}) - \mu \nabla \times \nabla \times \mathbf{u} \tag{2.2.37}$$

At this point, it is convenient to define the infinitesimal rotation of a rigid body w_{ij} as

$$w_{ij} = \frac{1}{2}\left(\frac{\partial u_j}{\partial x_i} - \frac{\partial u_i}{\partial x_j}\right) \tag{2.2.38}$$

or

$$\mathbf{w} = \tfrac{1}{2}\nabla \times \mathbf{u} \tag{2.2.39}$$

We note that $\mathbf{w}$ can be finite when the strain is zero, and vice versa. By substituting Eqs. (2.2.32) and (2.2.39) into Eq. (2.2.37) and using the relation $\nabla \cdot \mathbf{w} = \frac{1}{2}\nabla \cdot (\nabla \times \mathbf{u}) = 0$, we obtain the following separate wave equations for Δ and $\mathbf{w}$:

$$(\lambda + 2\mu)\nabla^2\Delta = \rho_{m0}\frac{\partial^2\Delta}{\partial t^2} \tag{2.2.40}$$

and

$$\mu\nabla^2\mathbf{w} = \rho_{m0}\frac{\partial^2\mathbf{w}}{\partial t^2} \tag{2.2.41}$$

respectively. These expressions are the general forms of the longitudinal and shear wave equations, respectively. Therefore, the longitudinal wave equation can be expressed entirely in terms of the dilation Δ, and the shear wave equation can be expressed entirely in terms of the rotation $\mathbf{w}$.

At this point it is convenient to use the fact that any vector can be written in terms of a vector potential and scalar potential. Thus the displacement vector $\mathbf{u}$ can be written in the form

$$\mathbf{u} = \nabla\phi + \nabla \times \boldsymbol{\psi} \tag{2.2.42}$$

where ϕ is a scalar potential and $\boldsymbol{\psi}$ is a vector potential. We shall show that the longitudinal wave solution can be stated entirely in terms of ϕ and that the shear wave solution can be stated entirely in terms of $\boldsymbol{\psi}$. All displacement components, as well as the stress and strain, can be determined in terms of ϕ and $\boldsymbol{\psi}$.

Longitudinal waves. We substitute Eqs. (2.2.32) and (2.2.42) into Eq. (2.2.40) and use the identity $\nabla \cdot (\nabla \times \boldsymbol{\psi}) = 0$ to obtain

$$\nabla^2\left[\rho_n \frac{\partial^2\phi}{\partial t^2} - (\lambda + 2\mu)\nabla^2\phi\right] = 0 \tag{2.2.43}$$

This expression is satisfied if erms in brackets are zero. Hence we can take the longitudinal wave equatic be

$$\rho_{m0}\frac{\partial^2\phi}{\partial t^2} - (\lambda + 2\mu)\nabla^2\phi = 0 \tag{2.2.44}$$

For waves that vary as $\exp[j(\omega t - \mathbf{k}_l \cdot \mathbf{r})]$, either Eq. (2.2.40) or Eq. (2.2.44)

leads to the result

$$k_l^2 \quad \text{———} \quad \omega^2 \tag{2.2.45}$$

Thus the longitudinal wave velocit relation

$$V_l = \sqrt{\lambda + 2\mu} = \sqrt{c_{11}} \tag{2.2.46}$$

By now this is a familiar result, but here we have proved that it holds for longitudinal wave propagation in an arbitrary direction in an isotropic solid, and that a pure longitudinal wave, uncoupled to a shear wave, can exist in an isotropic solid.

Shear waves. We now consider shear waves in an isotropic solid. Following a similar procedure to that used for longitudinal waves, we substitute Eqs. (2.2.39) and (2.2.42) into Eq. (2.2.41), and use the identity $\nabla x\ \nabla\phi = 0$, to obtain the relation

$$\nabla \times \nabla \times \left(\mu\nabla^2\psi - \rho_{m0}\frac{\partial^2\psi}{\partial t^2}\right) = 0 \tag{2.2.47}$$

Again, by assuming that the terms in parentheses are zero, we see that the shear wave equation is

$$\frac{\partial^2\psi}{} \quad \text{—}^2 \cdot \tag{2.2.48}$$

We obtain a one-dimensic m Eq. (2.2.41) or Eq. (2.2.48), with a solution of the form ex · a wave with velocity

$$V_s = \sqrt{\frac{\mu}{\rho_{m0}}} = \sqrt{\frac{c_{44}}{\rho_{m0}}} \tag{2.2.49}$$

2.2.4 Plane Wave Reflection and Refraction

We now consider the reflection of an infinite plane wave at a free surface. If a plane longitudinal or shear wave is normally incident on a free surface, the reflected wave will also be a wave of the same type and of equal amplitude. The boundary condition is that the normal component of stress at the surface is zero. It is easy to apply this condition in this simple case. More generally, if a longitudinal wave is incident in the x-y plane on a free surface $y = 0$ at an angle θ_{li} to the normal, as illustrated in Fig. 2.2.3, it will give rise to a reflected longitudinal wave at an angle θ_{lr} to the normal and a reflected shear wave at an angle θ_{sr} to the normal. The displacement associated with this shear wave will have a component in the vertical direction, so we call it a *shear vertical* wave.

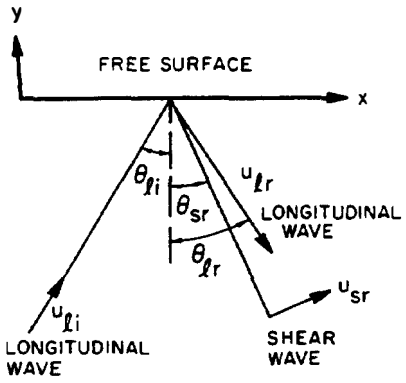

Figure 2.2.3 Longitudinal wave incident on a free surface. There are two reflected waves: a longitudinal wave and a shear wave.

The longitudinal wave can be represented in terms of a potential ϕ, which varies as $\exp(-j\mathbf{k}_l \cdot \mathbf{r})$. The incident longitudinal wave potential ϕ_{li}, in the coordinate system of Fig. 2.2.3, is defined as

$$\phi_{li} = A_{li} e^{-jk_l(x \sin \theta_{li} + y \cos \phi_{li})} \tag{2.2.50}$$

In the same way, there must be a reflected longitudinal wave ϕ_{lr} of the form

$$\phi_{lr} = A_{lr} e^{-jk_l(x \sin \theta_{lr} - y \cos \theta_{lr})} \tag{2.2.51}$$

and, in general, a reflected shear wave ψ_{sr} of the form

$$\psi_{sr} = A_{sr} e^{-jk_s(x \sin \theta_{sr} - y \cos \theta_{sr})} \tag{2.2.52}$$

where the potential ψ_{sr} is a vector in the z direction. Any other components in ψ_{sr} would give rise to additional components of $\mathbf{T}$ and $\mathbf{u}$, and thus would not satisfy the boundary conditions.

The boundary condition at the surface is that the total normal component of stress must be zero. Therefore, as shown in Sec. 1.5 and Appendix A, the stress components at the surface are

$$T_2 = T_{yy} = 0 \tag{2.2.53}$$

and

$$T_6 = T_{xy} = 0 \tag{2.2.54}$$

These stress components are derived as sums of the components of the longitudinal and shear waves. Thus, to satisfy the boundary conditions at any point along the surface $y = 0$, all components of the longitudinal and shear waves must have the same phase variation along the surface. This implies, from Eqs. (2.2.50)–(2.2.52), that

$$k_l \sin \theta_{li} = k_l \sin \theta_{lr} = k_s \sin \theta_{sr} \tag{2.2.55}$$

We conclude, just as we do for reflection of electromagnetic (EM) waves, that the angle of incidence equals the angle of reflection for the longitudinal waves, or

$$\theta_{li} = \theta_{lr} \tag{2.2.56}$$

We also arrive at the condition

$$\frac{\quad}{\sin} \quad - \quad - \quad \sqrt{\quad \mu} \tag{2.2.57}$$

This condition is like Snell's law for refraction of EM waves and is based on the same considerations. As $V_s < V_l$ in all isotropic solids, the reflected shear wave propagates at an angle closer to the normal than does the reflected longitudinal wave.

If we consider the opposite case of excitation by a shear vertical wave, we conclude, using the same type of notation, that

$$\frac{\sin \theta_{lr}}{\theta_{..}} = \frac{k_s}{k_l} = \frac{V_l}{V_s} \tag{2.2.58}$$

as illustrated in Fig. 2.2.4. Now the possibility exists that the angle θ_{lr} can become purely imaginary and that only a shear wave will be reflected if the angle of incidence of the shear wave is large enough. In this case, there will actually be a finite component of the reflected longitudinal wave, but its amplitude will fall off exponentially from the surface [4].

Incident longitudinal wave. We may solve for the amplitudes of the reflected waves by deriving the displacement and the stresses from the corresponding expressions for the potentials. For instance, for a longitudinal wave, incident on the plane $y = 0$, with amplitude varying as exp $(j\omega t)$, we can write $\mathbf{u} = -j\mathbf{k}_l A_{li}$ exp $(-j\mathbf{k}_l \cdot \mathbf{r})$. The two components of displacement are

$$u_x = \frac{\partial \phi}{\partial x} = -jk_l A_{li} \sin \theta_l e^{-jk_l(x \sin \theta_l + y \cos \theta_l)} \tag{2.2.59}$$

and

$$u_y = \frac{\partial \phi}{\partial y} = -jk_l A_{li} \cos \theta_l e^{-jk_l(x \sin \theta_l + y \cos \theta_l)} \tag{2.2.60}$$

It is also convenient, following Auld [7], to define an amplitude coefficient in terms of the displacement

$$\mathbf{u} = \frac{-\mathbf{k}_l}{k_l} A'_{li} e^{-j\mathbf{k}_l \cdot r} \tag{2.2.61}$$

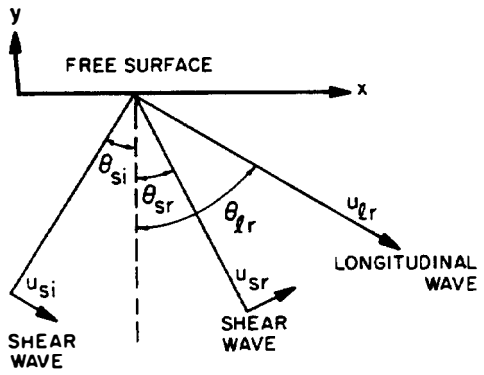

Figure 2.2.4 Shear wave incident on a free surface.

where the exp ($j\omega t$) variation is understood. Similarly, the reflected shear wave is generated from a potential $\boldsymbol{\psi}$ in the z direction, and we can write $\mathbf{u} = \nabla \times \boldsymbol{\psi}$. The two components of displacement are

$$u_x = \frac{\partial \psi_z}{\partial y} = jk_s A_{sr} \cos \theta_s e^{-jk_s(x \sin \theta_s - y \cos \theta_s)} \tag{2.2.62}$$

and

$$u_y = -\frac{\partial \psi_z}{\partial x} = jk_s A_{sr} \sin \theta_s e^{-jk_s(x \sin \theta_s - y \cos \theta_s)} \tag{2.2.63}$$

with

$$\mathbf{u} = j(\mathbf{k}_s \times \mathbf{a}_z) A'_{sr} e^{j\mathbf{k}_s \cdot \mathbf{r}} \tag{2.2.64}$$

and the reflected longitudinal wave is of the form $\mathbf{u} = j\mathbf{k}_l A_{lr} \exp(j\mathbf{k}_l \cdot \mathbf{r})$. It has components

$$u_x = -jk_l A_{lr} \sin \theta_l e^{-jkl(x \sin \theta_l - y \cos \theta_l)} \tag{2.2.65}$$

and

$$u_y = jk_l A_{lr} \cos \theta_l e^{-jkl(x \sin \theta_l - y \cos \theta_l)} \tag{2.2.66}$$

with

$$\mathbf{u} = \frac{\mathbf{k}_l}{k_l} A'_{lr} e^{j\mathbf{k}_l \cdot \mathbf{r}} \tag{2.2.67}$$

Writing $\mathbf{S} = \nabla_s u$ and $T = \mathbf{c}:\mathbf{S}$, we can now derive the stresses and strains corresponding to these waves. In general, by differentiating, we can show that both the longitudinal potential ϕ and the shear potential ψ give rise, in the x, y coordinate system, to longitudinal and shear components of stress. For instance, the longitudinal component of strain $S_1 = \partial u_x / \partial x$ has contributions from both ϕ and ψ, so at $x = 0$ and $y = 0$, we can write

$$S_1 = -k_l^2(A_{li} + A_{lr}) \sin^2 \theta_l + k_s^2 A_{sr} \sin \theta_s \cos \theta_s \tag{2.2.68}$$

Following Auld's treatment of the problem [7], we shall define reflection coefficients here in terms of the magnitude of the total displacements $\mathbf{u}$ or velocity $\mathbf{v} = j\omega\mathbf{u}$ of the waves, rather than in terms of the stress, as we did in Sec. 1.1. We write

$$\begin{aligned} \Gamma_{ll} &= \frac{A'_{lr}}{A'_{li}} \\ \Gamma_{sl} &= \frac{A'_{sr}}{A'_{si}} \end{aligned} \tag{2.2.69}$$

To solve for Γ_{ll} and Γ_{sl}, we employ the boundary conditions $T_2 = 0$ and $T_6 = 0$. We can use Eqs. (2.2.7) and (2.2.9) to write $T_2 = \lambda(S_1 + S_2) + 2\mu S_1$ and $T_6 = \mu S_6$. This gives two boundary conditions for two unknowns. Thus, for

longitudinal wave incidence, we can show (after some algebra) [7] that

$$\Gamma_{ll} = \frac{\sin 2\theta_s \sin 2\theta_l - (V_l/V_s)^2 \cos^2 2\theta_s}{\sin 2\theta_s \sin 2\theta_l + (V_l/V_s)^2 \cos^2 2\theta_s} \tag{2.2.70}$$

and

$$\Gamma_{sl} = \frac{2(V_l/V_s) \sin 2\theta_l \cos 2\theta_s}{\sin 2\theta_s \sin 2\theta_l + (V_l/V_s)^2 \cos^2 2\theta_s} \tag{2.2.71}$$

A curve, given by Auld, for a vertically polarized longitudinal wave reflected at the surface of fused quartz is shown in Fig. 2.2.5. Several interesting features of these results are apparent from the curves and the formulas used. As we might expect, at normal incidence ($\theta_l = 0$), $\Gamma_{ll} = 1$ and $\Gamma_{sl} = 0$.

Conversion of longitudinal to shear waves and shear to longitudinal waves. As the angle of incidence is increased, the longitudinal wave reflection coefficient Γ_{ll} decreases and a reflected shear wave begins to be excited, with Γ_{ll} initially increasing linearly with θ_l. At a certain point, the excitation of the reflected longitudinal wave may become zero; for fused quartz this occurs at $\theta_l = 42°$. Thus, for this condition, there is complete conversion from a longitudinal to a shear wave. This result is important because the phenomenon makes it possible to convert a longitudinal wave to a shear wave without losing power. As longitudinal wave transducers are often easier to construct than shear wave transducers, this is an extremely convenient method for obtaining shear waves. All that is required, as illustrated in Fig. 2.2.6, is a piece of fused quartz or another suitable material (see Prob. 11), cut to the correct angle.

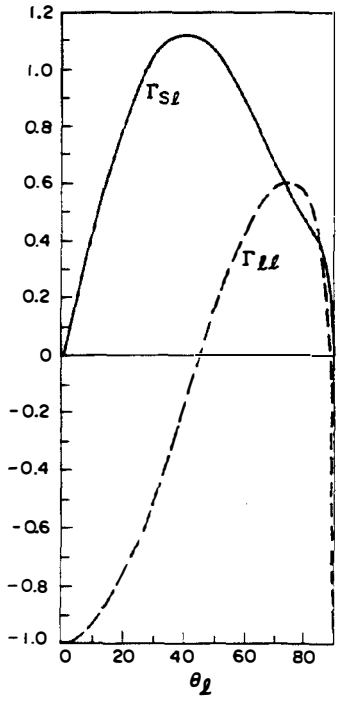

Figure 2.2.5 Reflection of a longitudinal wave at a stress-free boundary in fused silica. The vertical axis is the amplitude reflection coefficient defined in terms of the particle velocity. For fused quartz, $\sigma = 0.17$ and $V_s/V_l = 0.63$. (After Auld [7].)

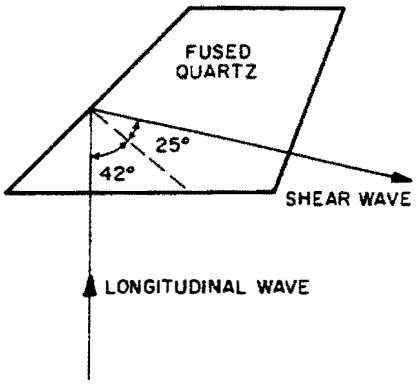

Figure 2.2.6 Longitudinal-to-shear wave converter using fused quartz. For fused quartz, $\sigma = 0.17$ and $V_s/V_l = 0.63$.

Note that the plot of Fig. 2.2.5 gives a maximum value of Γ_{sl} greater than unity. Because power flow normal to the surface is conserved, both the change in angle of incidence and reflection and the change in impedance for longitudinal and shear waves require that $\Gamma_{sl} \neq 1$ when Γ_{ll} is imaginary (see Prob. 10).

Because of reciprocity, the device also works in the opposite direction to convert a shear wave to a longitudinal one. A curve giving these results is shown in Fig. 2.2.7; note that at $\theta_s = 25°$, $\Gamma_{ss} = 0$. This phenomenon is, of course, closely analogous to the Brewster angle phenomenon in optics, although here it is used to convert one type of wave to another.

Another phenomenon we have already discussed is that when the angle of incidence of a shear wave is large enough, the angle of reflection of the longitudinal wave becomes greater than 90°. In this case, any longitudinal wave excited falls off exponentially in amplitude from the surface. Figure 2.2.7 shows that a shear wave incident at a fused quartz surface has a critical angle $\theta_{si} = \theta_{cr} = 41°$. Beyond this cutoff point, all incident shear wave power is converted to a reflected shear wave, so that $|\Gamma_{ss}| = 1$, although there is a π phase shift of Γ_{ss} as θ_s passes through the critical angle.

Beyond the longitudinal wave cutoff point, the amplitudes of the longitudinal wave components at the surface are indeed finite, but there is no real power

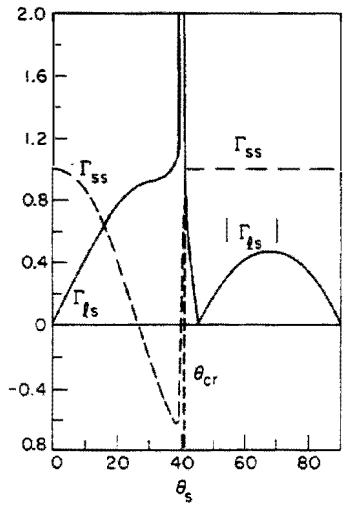

Figure 2.2.7 Reflection of a vertically polarized shear vertical wave at a stress-free boundary in fused silica. The vertical axis is the amplitude reflection coefficient defined in terms of the particle velocity. For fused quartz, $\sigma = 0.17$ and $V_s/V_l = 0.63$. (After Auld [7].)

associated with them. This implies that although $|\Gamma_{ls}|$ is finite, only decaying fields are associated with the longitudinal wave components near the surface.

Reflection and refraction. The same type of analysis can be carried out for refraction and reflection at the surface between two neighboring materials I and II, as illustrated in Fig. 2.2.8. Following the same arguments as before, the propagation constants of the reflected and refracted waves along the surface of the interface must be equal. This leads to a generalized Snell's law,

$$\sin \theta_{li} = \frac{V_{l\mathrm{I}}}{V_{s\mathrm{I}}} \sin \theta_{sr} = \frac{V_{l\mathrm{I}}}{V_{l\mathrm{II}}} \sin \theta_{lt} = \frac{V_{l\mathrm{I}}}{V_{s\mathrm{II}}} \sin \theta_{st} \tag{2.2.72}$$

which relates the angles of the various reflected and refracted rays.

The phenomenon of reflection and refraction is far more complicated for acoustic waves than for EM waves. The only simple case is that for an incident *shear horizontal* wave, a wave whose particle motion is parallel to a horizontal surface; as illustrated in Fig. 2.2.8, the particle motion is into the paper the figure is drawn on. In this case, all the boundary conditions are satisfied by stress components that arise only from shear horizontal waves; therefore, the reflected wave is also an shear horizontal wave. In the general case, the boundary conditions are more complicated, requiring several components of the relevant fields to be continuous across the boundary. The continuous components are: (1) the normal component of longitudinal stress; (2) the transverse component of shear stress; and (3) both the normal and transverse components of displacement. The amplitudes of the two transmitted and the two reflected waves can then be determined from the resulting equations.

This general case is similar in many ways to the simpler one of reflection at a free surface, which we discussed earlier in this section. Again, because of Snell's law, at certain critical angles no longitudinal wave is transmitted or reflected, depending on the wave velocities in the two media. As an example, consider the

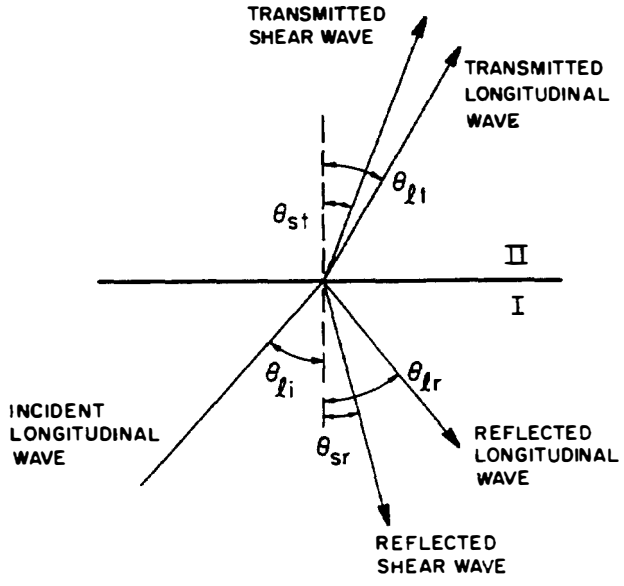

Figure 2.2.8 Refraction and reflection at the interface between two media.

longitudinal wave transmitted into aluminum from an incident longitudinal wave in water. The boundary conditions are simplified in this case because a shear wave cannot exist in water; thus there can be no reflected shear wave. Since the wave velocity in water is 1.5 km/s and the longitudinal wave velocity in aluminum is 6.42 km/s, there is no longer a refracted longitudinal wave in the aluminum if the incident wave in water reaches an angle θ_w greater than θ_{cr}, where $\sin \theta_{cr} = 1.5/6.42$ or $\theta_w \geq 13.5°$.

This phenomenon is extremely useful for looking at flaws in metals in nondestructive testing applications. To introduce a shear wave into the metal, the sample and the transducer are immersed in water. The transducer excites a longitudinal wave in the water, which, in turn, generally excites a longitudinal wave and a shear wave in the metal. If a flaw is present, a wave will be reflected from it. To obtain good definition, it is desirable to work with the shortest wavelength possible; thus shear waves are preferable to longitudinal ones because the shear wave velocity is approximately half the longitudinal wave velocity in most metals. Furthermore, some types of flaws, such as closed cracks, may show up better with shear wave excitation, which may cause one face of the crack to slip past the other. Using a beam incident from water to metal, we can excite a shear wave in a metal relatively easily; if we make the incident angle large enough, only a shear wave will be excited. Such techniques are commonly used, for instance, in nondestructive testing of nuclear reactor walls.

In Sec. 2.5 we show that this technique is also useful for exciting surface waves on metal. In this case, the wave of interest propagates along the surface (i.e., at 90° to the normal). Of course, we must know the propagation velocity of this wave along the surface to choose the incident angle correctly. Experimentally, the problem is relatively simple: It is a matter of rotating the transducer in the water until a wave of the desired type is excited.

Since both the shear and longitudinal wave velocities in aluminum (V_s = 3.04 km/s and V_l = 6.42 km/s) are larger than the longitudinal wave velocity in water (V_l = 1.5 km/s), there are two critical angles, one for each transmitted wave. Thus for angles of incidence larger than the shear critical angle (i.e., with $\theta_w >> \theta_{cr} = 29.6°$), the water–aluminum interface is a perfect reflector or mirror. The results of numerical calculations carried for this case are shown in Fig. 2.2.9.

Because power is conserved, it is often convenient to use transmission and reflection coefficients defined in terms of power rather than displacement, velocity, or stress. We have therefore used power reflection and transmission coefficients in Figs. 2.2.9–2.2.12. These coefficients are expressed in terms of the power density normal to the interface between the media (i.e., $P = Z|v|^2 \cos \theta/2$), where the parameters Z, θ, and v are appropriate to the wave of interest. For example, $T_{lw} = P_l/P_w$, where P_l is the power density normal to the interface associated with the longitudinal wave in aluminum and P_w is the power density normal to the interface of the incident wave in water. At normal incidence from the water, the power transmission coefficient to a longitudinal wave is $T_{lw} = 0.29$, while the power reflection coefficient is $R_{ww} = 0.71$ and the transmission coefficient to a shear wave is $T_{sw} = 0$. As the angle of incidence θ_w increases, T_{sw} increases and T_{lw} decreases to become zero at the critical angle. At an angle of incidence θ_w of approximately

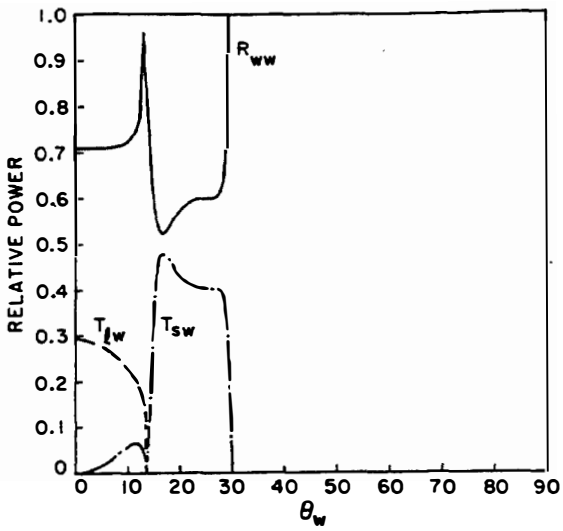

Figure 2.2.9 Plot of transmission and reflection coefficients as a function of the angle of incidence θ_w for a wave in water incident on aluminum. The transmission and reflection coefficients are defined in terms of power. For aluminum, $V_l = 6.42$ km/s, $V_s = 3.04$ km/s, and $\sigma = 0.355$.

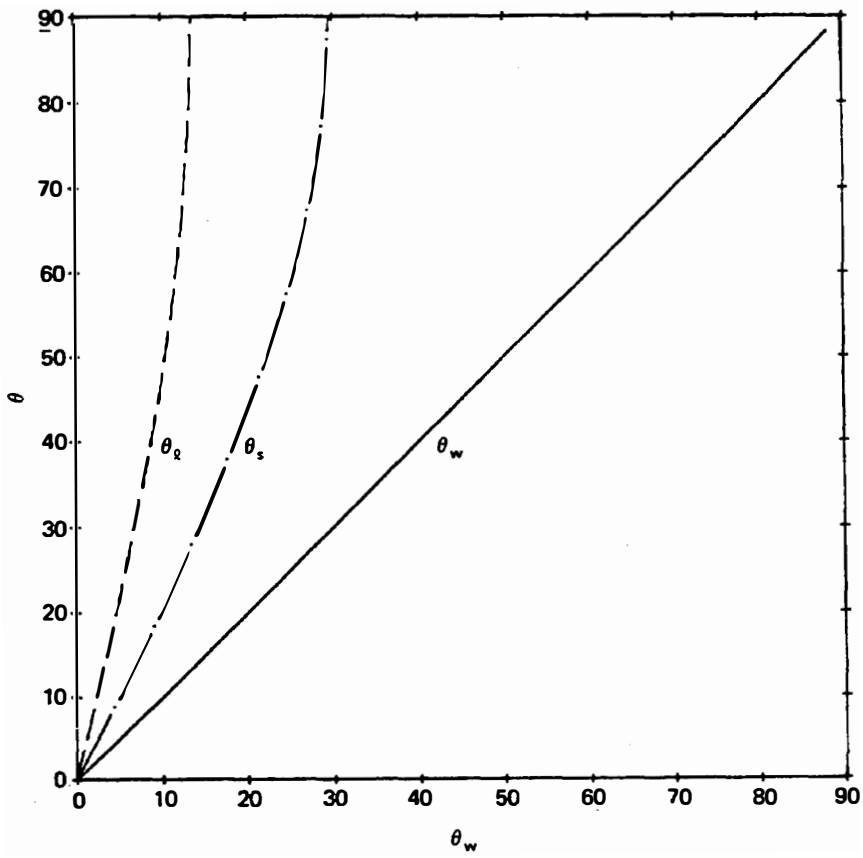

Figure 2.2.10 Plot of the relations of θ_w, θ_l, and θ_s for water and aluminum.

17°, almost half the incident power is converted to shear waves. Thus conversion to shear waves can be more efficient than conversion to longitudinal waves, because shear waves have a lower wave impedance. The relation between θ_s, θ_l, and θ_w is given in Fig. 2.2.10. The reverse situation, for conversion of longitudinal waves in aluminum to longitudinal waves in water, is shown in Fig. 2.2.11.

Another interesting use for a shear wave transducer is to excite a shear wave in a solid material such as aluminum, and to convert this wave, in turn, to a longitudinal wave in water. The curves in Fig. 2.2.12 show that approximately 40% of the incident energy can be converted to a longitudinal wave in water at incident angles for which the reflected longitudinal wave is cut off. Just as in the reverse case, transmission of a wave from water, the conversion ratio is better than for longitudinal wave excitation in the solid because the wave impedance of the shear wave is lower than that of a longitudinal wave.

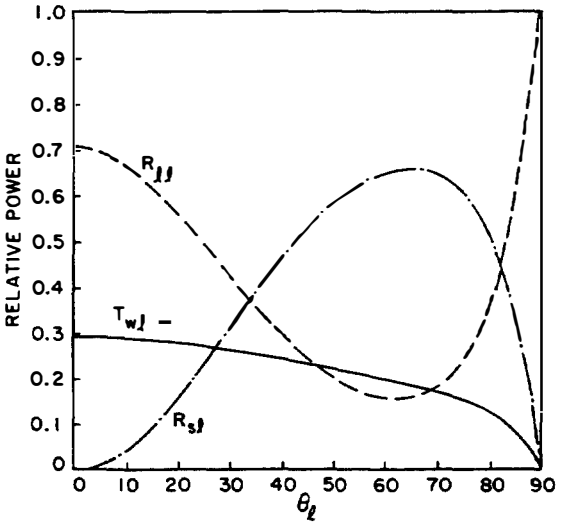

Figure 2.2.11 Plot of transmission and reflection coefficients as a function of incident angle θ_l for a longitudinal wave incident on a solid–water interface.

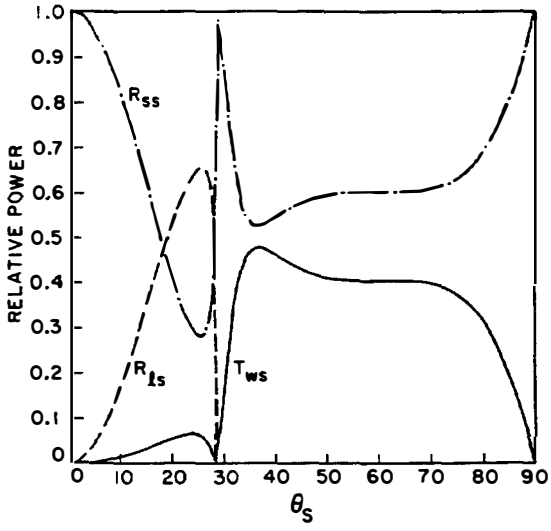

Figure 2.2.12 Plot of transmission and reflection coefficients as a function of incident angle θ_s for a shear wave incident on a solid–water interface.

PROBLEM SET 2.2

1. Consider the strip waveguide of isotropic material illustrated in the figure below:

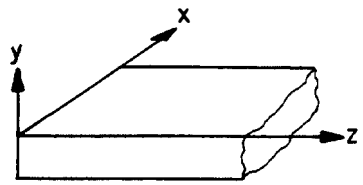

Regarding the guide as infinitesimally thin in the y direction and infinitely wide in the x direction, we expect that $T_2 = 0$ with $S_1 = 0$ and $u_x = 0$. Under these conditions, prove Eq. (2.2.26). Compare V_E/V_t and V_L/V_t for aluminum and crown glass.

2. Consider a PZT imaging array transducer element made of a thin strip regarded as infinitely long in the x direction, infinitesimally thin in the y direction, and finite in the z direction. This material is poled in the z direction and electrodes are deposited on its top and bottom surfaces.

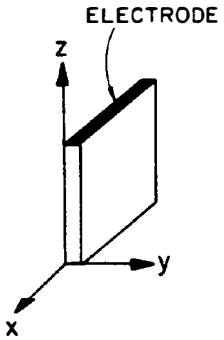

The transducer is designed to vibrate only in the z direction, and to have transverse resonances in the y direction of much higher frequency than the fundamental resonance in the z direction.

(a) Using the boundary conditions $T_2 = 0$, $S_1 = 0$, and $E_z = 0$ (i.e., there is no piezoelectric coupling), find the unstiffened acoustic velocity V_L^E in the z direction (see Prob. 1).

(b) Using the boundary condition $D_z = 0$, find the stiffened acoustic velocity V_L^D in the z direction and find an expression for the effective values of K^2 and k_T^2. Work out these values for PZT-5A.

Note. In this case, the material is anisotropic. You must assume that E_z and D_z are uniform (or zero) over any x-y plane, while D_z is independent of z. It will also be convenient to define a current per unit width, $I = j\omega \int D_z \, dy$.

3. Find c_{11}, c_{12}, and c_{44} in terms of s_{11}, s_{12}, and s_{44}.

4. Prove Eq. (2.2.37) by carrying out the complete derivation.

5. Consider a liquid in which $T_1 = T_2 = T_3 = -p$, where p is the pressure and $T_4 = T_5 = T_6 = 0$.

(a) Show that

$$\nabla p = -\rho_{m0}\ddot{\mathbf{u}}$$

(b) Find a wave equation for p, as well as the relation between p and the scalar longitudinal wave potential ϕ.

6. Derive Eqs. (2.2.70) and (2.2.71). Remember that $(V_l/V_s)^2 = (\lambda + 2\mu)/\mu$.
7. Derive the equivalents of Eqs. (2.2.70) and (2.2.71) for shear wave incidence.
8. We define a shear horizontal mode as one whose particle motion v_x is parallel to a surface of interest (see Sec. 2.3.2). Consider the transmission and reflection of a horizontal shear wave, with its propagation vector in the y-z plane, incident from an angle θ_i to the normal, to the interface $y = 0$ between two media with Lamé constants λ_1, μ_1 and λ_2, μ_2 and densities ρ_{m1} and ρ_{m2}, respectively. Show that the boundary conditions at the interface can be satisfied by shear horizontal modes in both media. Find the transmission and reflection coefficients for particle velocity v_x at the interface as a function of the incident angle θ_i, and the shear wave impedances of the two media.
9. Suppose that an incident longitudinal wave is converted completely to a shear wave, as illustrated in Fig. 2.2.6 and described by Eqs. (2.2.70) and (2.2.71). Suppose, in addition, that we require the exit wave to be at right angles to the incident wave (i.e., $\theta_s + \theta_l = \pi/2$). Find the condition on V_l/V_s for this to occur. What value of Poisson's ratio would the material need?
10. Power is conserved when an incident wave is reflected at an interface into shear and longitudinal wave components. Show that Eqs. (2.2.70) and (2.2.71) are consistent with this fact. You will need to consider carefully the power per unit area transmitted in the direction normal to the interface. Work out expressions for the power reflection coefficients R_{ll} and R_{sl}, using Eqs. (2.2.70) and (2.2.71), and define these parameters in terms of the power density normal to the interface.
11. Suppose that an incident longitudinal wave is converted completely to a shear wave, as illustrated in Fig. 2.2.6 and described by Eqs. (2.2.70) and (2.2.71).
    (a) By solving for V_l/V_s in terms of θ_s and then finding Poisson's ratio σ, show numerically that the range $V_l/V_s = 1.414$ to $V_l/V_s = 1.76$, with Poisson's ratio varying from 0 to 0.263, can satisfy the condition $\Gamma_{sl} = 0$. If $\sigma > 0.263$, however, it is not possible to satisfy the condition $\Gamma_{sl} = 0$.
    (b) Show that as $\sigma \to 0$, there are two possible solutions: $\theta_s \to 45°$ and $\theta_l \to 90°$ or $\theta_s \to 25.9°$ and $\theta_l \to 38.1°$.

2.3 ACOUSTIC WAVEGUIDES

2.3.1 Introduction

In this section we discuss the waves that can propagate in an acoustic waveguide. The modes involved in this case are more complicated than in the analogous electromagnetic (EM) waveguide, for even in a simple acoustic strip waveguide that has finite thickness in the y direction and is infinite in extent in the x and z directions, several different types of modes can exist. The simplest, which will be described in Sec. 2.3.2, is the *shear horizontal* mode, in which all particle motion is in the x direction and the wave is a pure shear wave. This mode is analogous to an EM waveguide mode. In Sec. 2.3.3 we describe Lamb waves, which have particle motion in both the y and z directions. Both shear and longitudinal wave components are needed to satisfy the boundary conditions of this mode. Finally, in Sec. 2.3.4 we describe surface acoustic waves, or Rayleigh waves, which propagate along the surface of a semi-infinite substrate. These waves have fields that

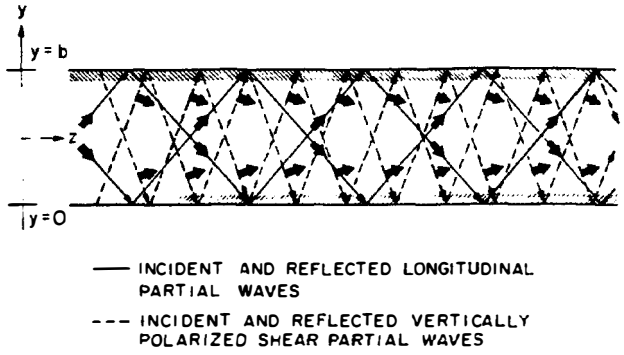

Figure 2.3.1 Partial wave pattern for transverse resonance analysis of Lamb wave propagation on an isotropic plate with free boundaries. (After Auld [7].)

fall off exponentially in amplitude away from the surface, and which need both shear and longitudinal wave components to satisfy the boundary conditions.

Consider a sheet of material of finite thickness b and infinite extent in the x and z directions, as illustrated in Fig. 2.3.1. If a shear wave is incident on the top surface from the inside of the material, it generally gives rise to both reflected shear and longitudinal waves, which, in turn, are reflected from the lower surface. Thus, in general, components of both shear and longitudinal waves will exist in the "waveguide," all of them with the same propagation constant β in the z direction, so as to satisfy the boundary conditions at all points on both surfaces. We will assume that the shear wave components are associated plane shear waves propagating at an angle to the z axis in the y-z plane. In the y, z coordinate system they must have fields that vary as $\exp(\pm jk_{sy}y) \exp(-j\beta z)$. By symmetry, the amplitudes of the waves incident on and reflected from the top surface must be equal. Consequently, the total shear wave potential must vary as $\psi = A \exp(-j\beta z) \sin(k_{sy}y + \alpha)$. Similarly, with the same assumptions, the longitudinal wave component must have a potential that varies as $\phi = B \sin(k_{ly}y + \gamma) \exp(-j\beta z)$, where α and γ are constants. In both cases we have assumed, for simplicity, that the field components have no variation in the x direction.

It follows from the wave equations for ϕ and ψ that

$$\beta^2 + k_{sy}^2 = k_s^2 \tag{2.3.1}$$

and

$$\beta^2 + k_{ly}^2 = k_l^2 \tag{2.3.2}$$

We must find the possible values of β for a given frequency ω (i.e., the eigenvalues of the waveguide modes). To do this, we must write the components of displacement, strain, and stress in the material in terms of the assumed forms of ϕ and ψ, and satisfy the boundary conditions at each surface.

2.3.2 Shear Horizontal Modes

We first consider the shear horizontal (SH) modes; these modes have only a u_x component, with ψ in the y direction and $\phi = 0$. As we assume only one component of ψ, ψ_y, we will, for simplicity, drop the subscript y and write

$$\psi = Ae^{-j\beta z} \cos(k_{sy}y + \alpha) \tag{2.3.3}$$

with

$$\frac{\partial \psi}{\quad} \qquad \beta \tag{2.3.4}$$

(2.3.5)

$$T_5 = T_{xz} = \mu \frac{\partial u_x}{\partial z} = \beta^2 A \mu e^{-j\beta z} \cos(k_{sy} y + \alpha) \tag{2.3.6}$$

and

$$T_6 = T_{xy} = \mu \frac{\partial u}{\partial y} \qquad j\beta_{sy} \mu A \qquad \beta \qquad \text{n}(k_{sy} y + \alpha) \tag{2.3.7}$$

The boundary condition is zero normal stress at the surface, that is, $T_6 = 0$ or $\sin(k_{sy} y + \alpha) = 0$ at $y = 0$, $y = b$. This implies that $\alpha = 0$ and

$$k_{sy} = \frac{n\pi}{b} \tag{2.3.8}$$

with

$$\psi = A e^{-j\beta z} \cos \frac{n\pi y}{b} \tag{2.3.9}$$

Thus there is a series of possible solutions or waveguide modes for different values of n, with corresponding values of β given by Eq. (2.3.1). In this case, we see that

$$\beta^2 = k_s^2 - \left(\frac{n\pi}{b}\right)^2 = \left(\frac{\omega}{V_s}\right)^2 - \left(\frac{n\pi}{b}\right)^2 \tag{2.3.10}$$

which is identical in form to the result for EM waveguides.

For β to be real for the nth mode, $\omega > n\pi V_s/b$ (i.e., there is a low-frequency cutoff for all but the $n = 0$ mode). If the frequency is less than this value, then β for the nth mode is imaginary and the wave does not propagate along the guide. Dispersion curves (plots of ω with respect to β) are given in Fig. 2.3.2. The phase velocity of the wave is

$$V_p = \frac{\omega}{\beta} \tag{2.3.11}$$

It follows from Eq. (2.3.10) that $V_p > V_s$ and that $V_p \to \infty$ at the cutoff frequency $\omega_{cn} = n\beta V_s/b$. Note also that the lowest mode $n = 0$ has a component of displacement only in the x direction and that the only finite component of stress is $T_5 = T_{xz}$ with no variation across the guide. In this case, the mode can propagate at all frequencies down to zero and its field components are like those of a plane shear wave mode propagating in the z direction. As we might expect, an SH plane wave propagating in the z direction in an infinite medium is not affected when the cross section of the medium is made finite in the y direction.

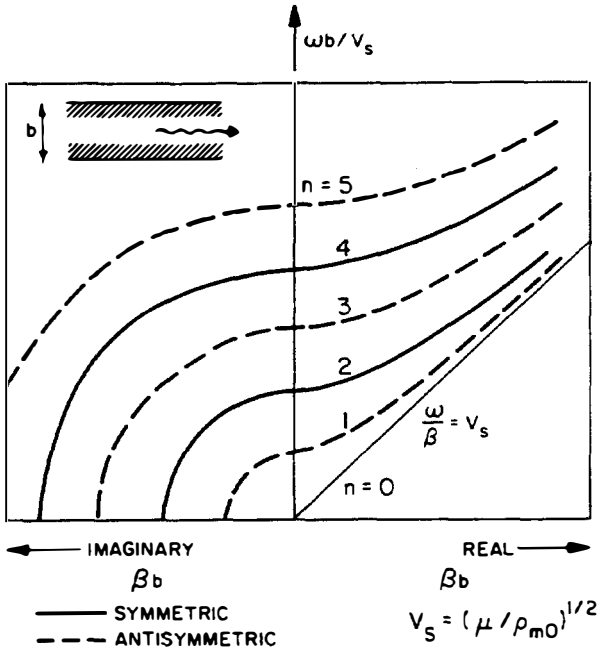

Figure 2.3.2 Dispersion curves for SH modes on an isotropic plate with free boundaries. (After Auld [7].)

2.3.3 Lamb Waves

A case of great practical interest is when the displacement is in both the y and z directions, so that ψ is in the x direction, ϕ is finite, and there are both shear and longitudinal components. The waves that exist in this case are known as *Lamb waves*. Some are primarily shear and others, primarily longitudinal, but both components are required to solve for the boundary conditions. In Sec. 2.2.1 we have already solved for one of these waves propagating in a very thin sheet; in that case, we assumed that the particle motion was essentially in the z direction with zero stress in the y direction. Our solution, with no variation of the displacement u_z across the sheet, was what is called the strip extensional mode of the system, that is, a mode that exists down to zero frequency with a phase velocity somewhat less than that of a longitudinal wave in an infinite medium. An analogous mode that exists down to zero frequency is a shear wave, called the flexural mode of the thin sheet. Higher-order modes, with several maxima and minima in the amplitude of variation of the field components across the guide, have a correspondingly higher frequency cutoff. We will not deal with the details of these waves here (see Problems 2.3.2 and 2.3.3). However, it is important to be aware of their existence and of the fact that their velocities can be calculated and measured experimentally. Furthermore, these waves can be excited from water or other media using an incident plane wave beam, incident at the correct angle, to excite the particular Lamb wave of interest. By measuring this critical angle for excitation of the Lamb wave, we can determine β, because for strong excitation, $\beta = k_{li} \sin \theta_{li}$ when k_{li} is the propagation constant of the incident wave. With this experimental technique, we can usually get a fairly good idea of the actual phase velocity of the Lamb wave $V_p = \omega/\beta$ along the waveguide.

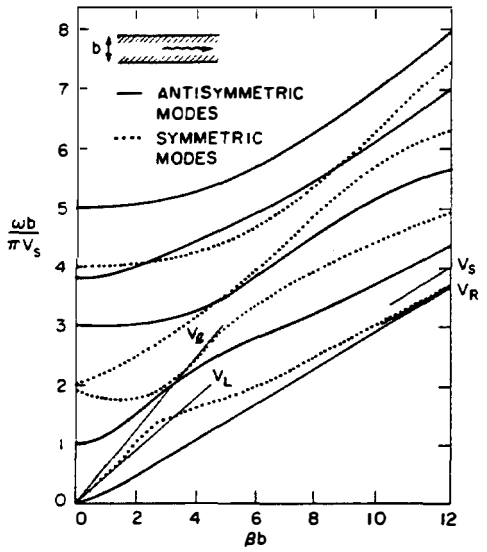

Figure 2.3.3 Lamb wave dispersion curves for the lower-order modes of an isotropic free plate with V_l/V_s = 1.9056. (After Auld [7].)

A plot of the dispersion curves for Lamb waves in a material such as aluminum is given in Fig. 2.3.3. The lowest-order symmetric mode (u_z is symmetric and u_y is antisymmetric about the central axis) extends down to zero frequency (see Probs. 2 and 3). This mode, as we have seen, has a phase velocity V_L that is lower than that for a longitudinal wave as $\omega \rightarrow 0$. As the frequency is increased, the phase velocity increases and approaches the longitudinal wave velocity. It then decreases again until it approaches the Rayleigh wave velocity, which is a little less than the shear wave velocity. When $\beta b >> 1$, the value of u_z at the center of the guide becomes less than at the edges. Thus, at very high frequencies, the mode looks like two surface acoustic waves, or Rayleigh waves (which will be discussed in Sec. 2.3.4), propagating along the boundary surfaces of the guide.

There is also a lowest-order antisymmetric mode or *flexural mode* (u_z is antisymmetric and u_y is antisymmetric about the central axis) extending down to zero frequency. The velocity of this flexural mode is usually lower than the shear wave velocity and the Rayleigh wave velocity.

2.3.4 Surface Waves

We have now briefly discussed the different types of waves that can exist in a solid medium of finite width. In this section we devote considerable attention to Rayleigh waves. These are waves of great technical importance that exist only near the surface of a semi-infinite medium. For this reason such waves are called surface waves. A familiar example of a surface wave is one that propagates along the surface of water. In this case, the wave motion is strong at the surface of the water and falls off very rapidly into its interior. In a water wave, the inertial forces are associated with the mass of the water and the restoring forces are due to gravity, rather than Hooke's law.

When scientists first began to analyze seismic motions of the earth, they noted that when a distant disturbance occurs, an observer notes three distinct events.

The first is a result of longitudinal waves propagating through the interior of the earth. The second is due to shear waves, which, because they propagate at a slower velocity than longitudinal waves, reach the observer at a later time. Finally, a third disturbance, due to a wave propagating along the curved surface of the earth, reaches the observer; this surface wave disturbance is the strongest of the three.

Lord Rayleigh proposed a theory for the surface wave, which shows that it consists of a mixture of shear and longitudinal stress components [8]. Because there is no restoring force at the surface of a solid medium, any force normal to the surface must be zero. Thus the boundary condition at the surface is that the normal components of stress must be zero. If a wave propagating in the z direction exists in a semi-infinite medium, the total energy per unit length in the wave must be finite. This, in turn, implies that the field components associated with the wave will fall off exponentially into the interior of the medium. As we shall see, we can indeed obtain a mathematical solution that satisfies the boundary conditions.

Surface acoustic waves are technically important because their energy is concentrated in a relatively small region, approximately one wavelength deep, near the surface. The waves are therefore accessible from the surface. Thus Rayleigh waves produced by seismic disturbances are the ones most easily detected by sensors on the surface of the earth [3, 6, 8–13].

If the medium is piezoelectric, the electric fields associated with the wave should be stronger near the surface. Consequently, by depositing electrodes on the surface of a piezoelectric material, a surface wave can be excited or detected relatively easily. Furthermore, it is also easy to sample the wave along its path (i.e., to make taps for a surface wave delay line). The technology is inexpensive and convenient because the electrodes required to excite or detect these waves can be deposited by the standard techniques used for photolithography of integrated circuits.

Rayleigh waves in an isotropic medium. We consider a medium that is semi-infinite in the $-y$ direction with a free surface at $y = 0$ and particle displace-

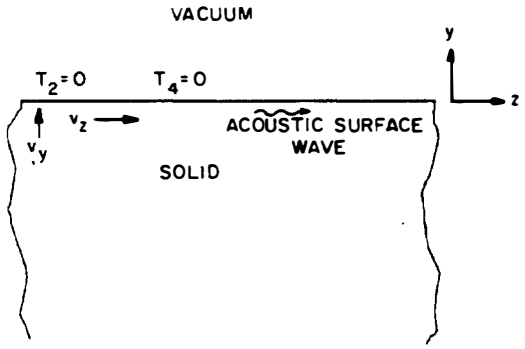

Figure 2.3.4 Configuration for acoustic surface wave analysis.

ment only along the y and z axes, as illustrated in Fig. 2.3.4. We use Eqs. (2.2.44) and (2.2.48) and write the wave equations for the potentials in the following forms:

$$\frac{\partial^2\phi}{\partial z^2} + \frac{\partial^2\phi}{\partial y^2} + k_l^2\phi = 0 \tag{2.3.12}$$

and

$$\frac{\partial^2\boldsymbol{\psi}}{\partial z^2} + \frac{\partial^2\boldsymbol{\psi}}{\partial y^2} + k_s^2\boldsymbol{\psi} = 0 \tag{2.3.13}$$

where

$$\begin{aligned} k_l &= \omega\sqrt{\frac{\rho_{m0}}{\lambda + 2\mu}} \\ k_s &= \omega\sqrt{\frac{\rho_{m0}}{\mu}} \end{aligned} \tag{2.3.14}$$

The motion is assumed to be independent of the coordinate x. Thus only the component of the vector potential $\boldsymbol{\psi}$ along the x axis will be finite, and we write $\boldsymbol{\psi} = \mathbf{a}_x\psi$. If, as in Sec. 2.2.3, we associate the potential ϕ with the longitudinal component of motion, and the potential ψ with the shear waves, we can write the following relations:

$$u_z = \frac{\partial\phi}{\partial z} - \frac{\partial\psi}{\partial y} \tag{2.3.15}$$

$$u_y = \frac{\partial\phi}{\partial y} + \frac{\partial\psi}{\partial z} \tag{2.3.16}$$

$$T_1 = \lambda\left(\frac{\partial^2\phi}{\partial y^2} + \frac{\partial^2\phi}{\partial z^2}\right) \tag{2.3.17}$$

$$T_2 = \lambda\left(\frac{\partial^2\phi}{\partial y^2} + \frac{\partial^2\phi}{\partial z^2}\right) + 2\mu\left(\frac{\partial^2\phi}{\partial y^2} + \frac{\partial^2\psi}{\partial y\,\partial z}\right) \tag{2.3.18}$$

$$T_3 = \lambda\left(\frac{\partial^2\phi}{\partial y^2} + \frac{\partial^2\phi}{\partial z^2}\right) + 2\mu\left(\frac{\partial^2\phi}{\partial z^2} - \frac{\partial^2\psi}{\partial y\,\partial z}\right) \tag{2.3.19}$$

and

$$T_4 = \mu\left(2\frac{\partial^2\phi}{\partial y\,\partial z} + \frac{\partial^2\psi}{\partial z^2} - \frac{\partial^2\psi}{\partial y^2}\right) \tag{2.3.20}$$

We seek solutions for both the shear and longitudinal terms, which have the same phase variation in the z direction. Thus we can write ϕ as

$$\phi = F(y)e^{j(\omega t - \beta z)} \tag{2.3.21}$$

and ψ as

$$\psi = G(y)e^{j(\omega t - \beta z)} \tag{2.3.22}$$

Substituting Eqs. (2.3.21) and (2.3.22) into Eqs. (2.3.12) and (2.3.13), respectively, leads to the following results:

$$\frac{d^2F}{dy^2} = (\beta^2 - k_l^2)F(y) \tag{2.3.23}$$

and

$$\frac{d^2G}{\partial y^2} = (\beta^2 - k_s^2)G(y) \tag{2.3.24}$$

We look for surface wave solutions where the components fall off exponentially to $y = -\infty$ so that they have finite stored energy per unit length. We take $F(y)$ to vary as exp $(\gamma_l y)$ and $G(y)$ to vary as exp $(\gamma_s y)$. From Eqs. (2.3.23) and (2.3.24), it follows that

$$\gamma_l^2 = \beta^2 - k_l^2 \tag{2.3.25}$$

and

$$\gamma_s^2 = \beta^2 - k_s^2 \tag{2.3.26}$$

The solutions for ϕ and ψ must take the forms

$$\phi = Ae^{-j\beta z}e^{\gamma_l y} \tag{2.3.27}$$

and

$$\psi = Be^{-j\beta z}e^{\gamma_s y} \tag{2.3.28}$$

respectively. The boundary condition of the problem is that the normal component of stress at the surface must be zero. In turn, this implies that T_2 and T_4 are zero at the surface. We substitute Eqs. (2.3.27) and (2.3.28) into Eqs. (2.3.18) and (2.3.20) to write

$$T_4 = \mu[-2j\beta\gamma_l Ae^{\gamma_l y} - (\beta^2 + \gamma_s^2)Be^{\gamma_s y}]e^{-j\beta z} \tag{2.3.29}$$

and

$$T_2 = \mu[A(\gamma_s^2 + \beta^2)e^{\gamma_l y} - 2jB\beta\gamma_s e^{\gamma_s y}]e^{-j\beta z} \tag{2.3.30}$$

The condition that $T_4 = 0$ and $T_2 = 0$ at $y = 0$ imply that

$$B = -\frac{2j\beta\gamma_l A}{} \tag{2.3.31}$$

and

$$A = \frac{}{\beta^2 + \gamma_s^2} \tag{2.3.32}$$

Substituting Eq. (2.3.32) into Eq. (2.3.31), we obtain one form of the Rayleigh wave dispersion relation:

$$4\beta^2\gamma_l\gamma_s - (\beta^2 + \gamma_s^2)^2 = 0 \tag{2.3.33}$$

Substituting Eqs. (2.3.25) and (2.3.26) into Eq. (2.3.33), we can also write the Rayleigh wave dispersion relation as a cubic equation in β^2. We then write the dispersion relation in terms of the Rayleigh wave velocity $V_R = \omega/\beta$, in the form

$$\left(\frac{V_R}{V_s}\right)^6 - 8\left(\frac{V_R}{V_s}\right)^4 + 8\left[3 - 2\left(\frac{V_s}{V_l}\right)^2\right]\left(\frac{V_R}{V_s}\right)^2 - 16\left(1 - \frac{V_s}{V_l}\right)^2 = 0 \tag{2.3.34}$$

where V_s, V_l, and V_R are the shear wave velocity, the longitudinal wave velocity, and the Rayleigh wave velocity, respectively. This dispersion relation has a real root, the *Rayleigh root*, which can be stated in the approximate form [7, 10] (see Prob. 6) as

$$\frac{k_s}{\beta} = \frac{V_R}{V_s} \approx \frac{0.87 + 1.12\sigma}{1 + \sigma} \tag{2.3.35}$$

The Rayleigh wave is a nondispersive wave, with V_R varying from $0.87V_s$ to $0.95V_s$ as Poisson's ratio varies from 0 to 0.5. A plot of V_R/V_s as a function of V_s/V_l is compared with the approximate solution in Fig. 2.3.5.

Note that we have neglected two other roots of the dispersion relation. These correspond to waves propagating from $y = -\infty$, which are reflected from the surface (see Prob. 7).

The Rayleigh wave velocity V_R is always less than the shear wave velocity V_s or the longitudinal wave velocity V_l. This is necessary because for the waves to fall off in amplitude exponentially into the interior of the medium, γ_l and γ_s must be real, and hence $k_r > k_l$ and $k_r > k_s$. We have already seen that the shear wave velocity is always less than the longitudinal wave velocity. Consequently, the Rayleigh wave velocity must always be considerably less than the longitudinal wave velocity but only slightly less than the shear wave velocity. Because the Rayleigh wave velocity is closest to the shear wave velocity, most of the stored energy in the medium is associated with shear wave components, rather than the longitudinal ones; thus in many respects the Rayleigh wave behaves like a shear wave. So

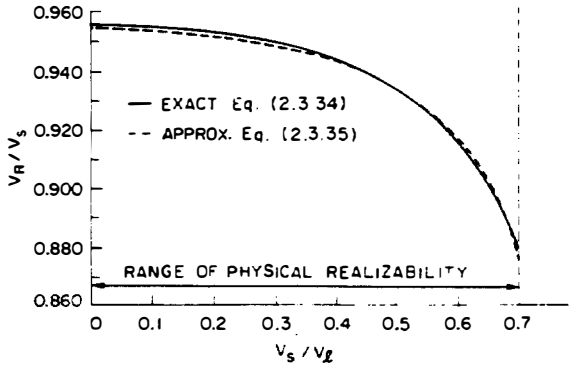

Figure 2.3.5 Isotropic Rayleigh wave velocity V_R as a function of the bulk shear wave velocity V_s and the bulk longitudinal wave velocity V_l. (After Auld [7].)

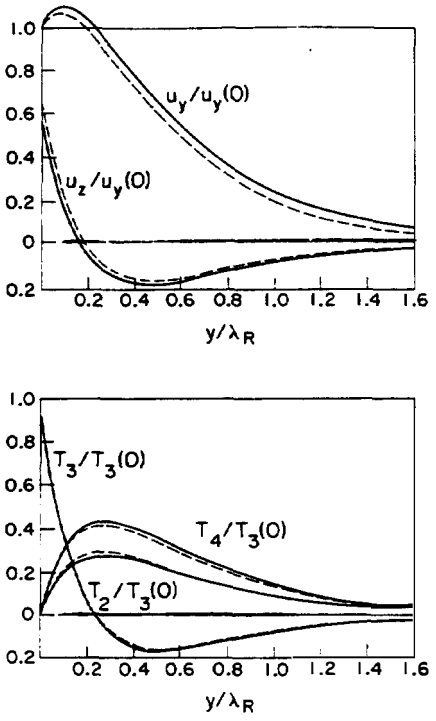

Figure 2.3.6 Plot of the normalized values of stress and displacement components of a Rayleigh wave: solid lines, $\sigma = 0.34$; dashed lines, $\sigma = 0.25$.

when surface roughness or air loading are not dominant effects, the Rayleigh wave attenuation is comparable to that of shear wave loss in most materials. The way the Rayleigh wave velocity varies with the angle of propagation relative to the crystal axis in an anisotropic crystal also follows fairly closely to the way the shear wave velocity varies with direction.

The displacement and stress components of the wave do not fall off as simple exponentials into the interior of the medium because both the longitudinal and shear potentials ϕ and ψ contribute to these components. Thus it follows from Eqs. (2.3.27)–(2.3.32) that

$$T_4 = -2jA\gamma_l\mu A(e^{\gamma_l y} - e^{\gamma_s y}) \tag{2.3.36}$$

and

$$T_2 = \mu A(\gamma_s^2 + \beta^2)(e^{\gamma_l y} - e^{\gamma_s y}) \tag{2.3.37}$$

Hence T_4 and T_2 increase from an initial zero to fall off finally as $e^{\gamma_s y}$ into the interior. A plot of how some of the important components vary with y is given in Fig. 2.3.6.

PROBLEM SET 2.3

1. Consider a layered material with a shear wave elastic constant μ_1, density ρ_{m1}, and a thickness h, laid down on a semi-infinite substrate with a shear wave elastic constant μ_2 and density ρ_{m2}. A type of SH wave known as a *Love* wave can propagate in this

configuration. To have finite energy, its fields must fall off exponentially in the $-y$ direction in the semi-infinite substrate. This wave is dispersive (i.e., the phase velocity varies with frequency).

Take u_x to vary as $\cos(k_y y + \alpha) \exp(-j\beta z)$ in the upper layer and as $\exp(\gamma y) \exp(-j\beta z)$ in the substrate, the interface between the layers to be at $y = 0$, and all field components to be invariant with x, with

$$k_y^2 = k_{s1}^2 - \beta^2$$

$$\gamma^2 = \beta^2 - k_{s2}^2$$

and

$$k_{s1}^2 = \frac{\omega^2 \rho_{m1}}{\mu_1}$$

$$k_{s2}^2 = \frac{\omega^2 \rho_{m2}}{\mu_2}$$

In this case, unlike that of the simple SH mode guide, note that k_y is a variable that changes with frequency.

(a) By matching the boundary conditions at the interface and using the boundary conditions at the top surface, find a transcendental relation between γ and k_y (the dispersion relation) from which, with the relations already given, β may be found. Show that the media must be chosen so that $k_{s2} < k_{s1}$.

(b) Show that for the lowest mode the fields extend to $y = -\infty$ as $\omega \to 0$. What is the relation between β and k_{s2} and hence the phase velocity ω/β of the wave at this point? Find the high-frequency limit of this mode where $\beta \to \infty$ and $\gamma \to \infty$. What is the relation between β and k_{s1} at this point? What is the phase velocity of this mode at the high-frequency limit? Sketch how $k_y b$ varies with frequency, as well as the ω–β relation for the lowest-order mode. You will find it convenient to consider $\tan(k_y b)$ and its limits as $k_y b \to 0$ and $k_y b \to \pi/2$.

(c) Find the value of $k_y b$ when $\gamma = 0$ for the next mode of the Love wave, as well as an expression for the low-frequency cutoff of this wave.

2. (a) Assume that a symmetrical Lamb wave has ϕ, an even function of y, and ψ_x, an odd function of y, about the center of a strip of thickness b. Find a transcendental expression from which the propagation constant β may be found. Show that as $\omega \to 0$, the transverse propagation constants in the y direction of the lowest order mode also approach zero. Show that in this case the phase velocity of the wave V_p approaches V_L, which is defined in Eq. (2.2.26), or by Prob. 2.2.1. Assume that both ϕ and ψ vary as $\exp(-j\beta z)$. Follow the methods suggested in Prob. 1.

Note. As $\omega \to 0$, $k_s \to 0$, $k_l \to 0$, and $\beta \to 0$, so $k_{sy} \to 0$ and $k_{ly} \to 0$.

Answer.

$$\frac{\tan(k_{sy} b/2)}{\tan(k_{ly} b/2)} = -\frac{4\beta^2 k_{sy} k_{ly}}{(k_{sy}^2 - \beta^2)^2}$$

where $k_{sy}^2 = k_s^2 - \beta^2$, $k_{ly}^2 = k_l^2 - \beta^2$, $k_s^2 = \omega^2 \rho_{m0}/\mu$, and $k_l^2 = \omega^2 \rho_{m0}/(\lambda + 2\mu)$.

3. Consider the antisymmetric Lamb wave with ϕ, an odd function of y, and ψ_x, an even function of y, about the center of a strip of thickness b, using the methods suggested in Prob. 2.

(a) Find a transcendental expression from which the propagation constant may be found.

Answer.

$$\frac{\tan (k_{sy}b/2)}{\tan (k_{ly}b/2)} = -\frac{(k_{sy}^2 - \beta^2)^2}{4\beta^2 k_{sy}k_{ly}}$$

with the same definitions as in Prob. 2.

(b) Find the phase velocity of the antisymmetric mode as $\omega \to 0$. Assume that both ϕ and ψ vary as $\exp(-j\beta z)$. Show that as $\omega \to 0$, the group velocity is twice the phase velocity, where the phase velocity is $V_p = \omega/\beta$ and the group velocity is $V_g = d\omega/d\beta$.

Answer.

$$(\beta b)^4 = \frac{3k_s^2 b^2}{1 - (k_l/k_s)^2} \qquad V_p = \frac{\omega}{\beta}$$

Note. You will need to expand the trigonometric functions to third order in the argument to find this relation. For a thin strip, look for a solution where $\beta \to 0$ less slowly than k_l or k_s, as can be seen from final result (i.e., neglect k_l^2 or k_s^2 compared to β^2). Do not neglect k_{sy}^2 relative to β^2 as $(\beta b)^2 \to 0$.

4. (a) Show from general considerations based on Eq. (2.2.21) that at $y = 0$, the Rayleigh wave components satisfy the relation $T_1(0) = \sigma T_3(0)$. Using Eq. (2.2.21) and the symmetric expressions for S_2 and S_3, find $S_2(0)$ and $S_3(0)$ in terms of $T_3(0)$.

(b) Using Eqs. (2.3.17) and (2.3.19), find expressions for $T_1(y)$ and $T_3(y)$ and show that your results also yield $T_1(0) = \sigma T_3(0)$.

5. Find the total power flow in the z direction associated with the propagation of a Rayleigh wave. Show that if v_y is the RF velocity at $y = 0$, then for a beam of width w,

$$\frac{v_y v_y^*}{P} = \frac{f_y \omega}{w\rho_{m0}V_s^2}$$

where

$$f_y = \frac{4\gamma^2[1 - (V_R j/V_s)^2]^{3/2}}{3\gamma - 2\gamma(V_R/V_s)^2 - 1}\left(\frac{V_s}{V_R}\right)^2$$

and

$$\gamma^2 = \frac{1 - (V_R/V_l)^2}{1 - (V_R/V_s)^2}$$

and V_R, V_s, and V_l are the Rayleigh wave, shear wave, and longitudinal wave velocities, respectively.

6. Prove the approximate result of Eq. (2.3.35) by putting $\beta = k_s(1 + \Delta)$ in Eq. (2.3.33) and keeping only first-order terms in Δ.

Answer.

$$\frac{k_s}{\beta} = \frac{0.875 + 1.125\,\sigma}{1 + \sigma}$$

7. Consider the solutions of Eq. (2.3.34) with $\sigma = 0.25$. In this case show that $(V_l/V_s)^2 = 3$ and that there are three real solutions of the Rayleigh wave equations: $(V_R/V_s)^2 =$

4, $2 + 2/\sqrt{3}$, and $2 - 2/\sqrt{3}$. The last root is the normal Rayleigh root with $V_R/V_s = 0.9194$.

(a) Discuss the first root, which corresponds to a velocity $V_R > V_l$. Is it a true root of the equation? Find the values of γ_l and γ_s that satisfy Eq. (2.3.33). Compare your results with the situation for a longitudinal wave incident at an angle θ_l to the normal and giving rise to only a reflected shear wave. Find θ_l and θ_s, the reflected wave angle. You may find it useful to make use of Eqs. (2.2.70) and (2.2.71) in your discussion.

(b) Find θ_l and θ_s for the second root of Eq. (2.3.33).

2.4 INTERDIGITAL TRANSDUCERS

2.4.1 Introduction

The major advantage of surface acoustic waves is simply that they are accessible at the surface; thus surface acoustic wave (SAW) devices can be easily adapted to the technology developed for creating microcircuits in thin, flat structures. In typical applications, most of the acoustic energy is contained within 1 to 100 μm from the surface. A surface acoustic wave can be easily excited anywhere on the surface and readily received elsewhere on the same "chip." Thus it is easy, as well as desirable, to construct a delay line in which an acoustic wave travels along the surface of the crystal rather than through its interior. Because the wave is so easily accessible, signals with different delay times can be picked up at various points along their path; thus the delay line can be tapped at several intermediate points to create a *transversal filter*. Chapter 4 deals with the theory of such filters in detail.

In recent years, the technology of acoustic wave devices has expanded rapidly, due to the development of *interdigital transducers*, which convert an electrical signal into a surface acoustic wave and reconvert it into an electrical signal. This type of transducer, illustrated in Fig. 2.4.1, is normally used to excite a surface acoustic wave on a piezoelectric material.

We can produce an electric field at the surface of a piezoelectric crystal by applying an electrical potential to two parallel metal electrodes deposited on it, as shown in Fig. 2.4.1(a). This field excites a surface acoustic wave that can be reconverted to an electrical signal at a second similar pair of electrodes laid down on the piezoelectric substrate. But a single pair of electrodes cannot excite surface acoustic waves very efficiently, so instead, it is customary to use an interdigital transducer consisting of several pairs of electrodes or fingers, placed one after the other in an interdigital pattern, as shown in Fig. 2.4.1(b). Thus each pair of electrodes excites a Rayleigh wave, and the transducer is designed so that these separately excited waves reinforce one another and give rise to a usefully large acoustic signal. This is accomplished by choosing the spacing between each finger pair so that a Rayleigh wave travels that distance in exactly the time required for the exciting signal to repeat itself (i.e., the finger pair spacing is one wavelength).

If the frequency of the wave is altered from this ideal value, the individual excitations from each pair of fingers will have a tendency to cancel each other out.

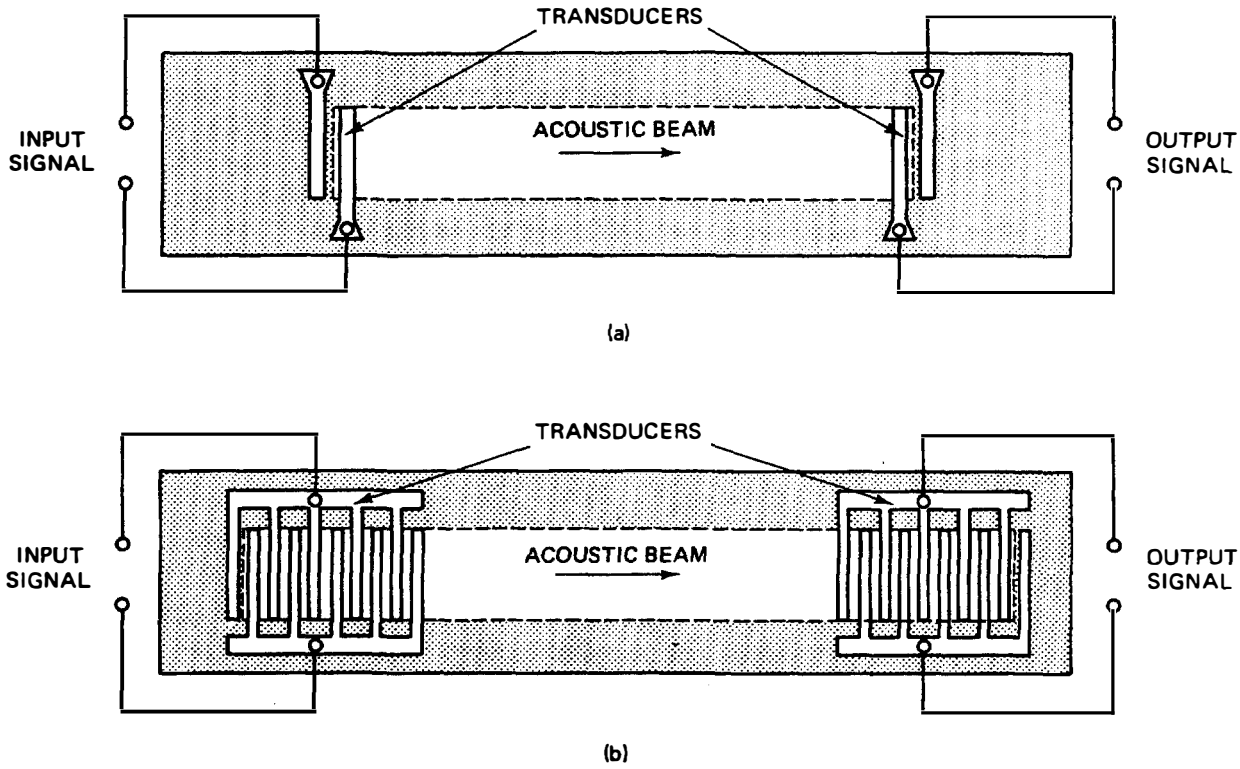

Figure 2.4.1 Excitation and detection of Rayleigh waves: (a) by a simple interdigital transducer consisting of two metal electrodes deposited on a piezoelectric crystal; (b) by a multiple-finger interdigital transducer. (After Kino and Shaw [14].)

The longer the transducer, and hence the more fingers it has, the more easily a slight change in frequency will cause the signal from one end of the transducer to be out of phase with the signal excited at the other end. Thus a long transducer with many fingers tends to be efficient for exciting and receiving signals only over a narrow frequency range and can also act as a filter to differentiate signals of one frequency from signals of another. Conversely, a short transducer with only a few fingers can be used to excite signals over a wider frequency range.

Figure 2.4.2 shows the performance of one of the first efficient SAW delay lines, of the type shown in Fig. 2.4.1(b), fabricated on the surface of a lithium niobate crystal. Each interdigital transducer consists of five identical finger pairs with finger widths and spacings of 8 μm; this gives a center frequency of operation of 105 MHz. These dimensions are scaled inversely with frequency.

Filters of this kind are commonly used in communication systems. A television receiver, for example, must be able to switch among several channels, each of which is at a different frequency; thus it requires several individual filters corresponding to the frequency of each channel. The signal from the chosen channel is then shifted to an "intermediate" frequency and passed through another filter that separates the picture and sound information, as well as strongly rejecting signals from the adjacent channels. SAW filters are now widely used as intermediate-frequency (IF) filters in this application.

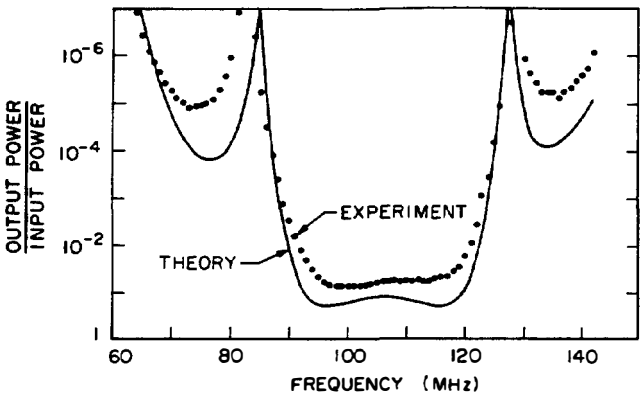

Figure 2.4.2 Bandpass frequency response of an early two-port SAW delay line. (After Smith et al. [11].)

The interdigital transducers used to generate and detect surface acoustic waves are extremely small. For example, if we want to excite waves with a frequency of 40 MHz, then each finger can be no more than about 20 μm wide and the spacing between them must be of comparable dimensions, since the finger pair spacing should be one wavelength. Lithium niobate, a typical material used in this application, has a Rayleigh velocity of 3.3 km/s. Thus for 40 MHz, $\lambda \sim 80$ μm. A frequency near 40 MHz is a common intermediate frequency in television applications. To excite waves with a frequency of 1 GHz, the fingers must be spaced by one twenty-fifth of this distance, or 0.8 μm. Transducers with such dimensions can be produced by the well-developed photolithographic techniques commonly used in the semiconductor industry. In practice, the metal fingers are deposited on the crystal by evaporating, in a high vacuum, a metal such as gold or aluminum through a suitably exposed photoresist mask. The mask through which the photoresist layer is exposed is itself made photographically, by reducing a large-scale reproduction of the interdigital transducer by a factor on the order of 100. This means that many identical filters can be produced by relatively simple and inexpensive photographic techniques.

2.4.2 Delta-Function Model of the Transducer

We can use a simple mathematical model to represent the excitation of a Rayleigh wave by an SAW transducer. We consider the excitation by an individual finger to be proportional to the total charge Q on the finger. Suppose that all the fingers are of equal length w in the x direction across the acoustic beams, and that the charge density per unit length in the direction of acoustic propagation z at z' on the surface of the piezoelectric material is $\sigma(z')$, as shown in Fig. 2.4.3. Because the system is linear, the SAW signal excited by the charge in a length dz' is proportional to $\sigma(z')dz'$. This surface acoustic wave has a propagation constant $k = \omega/V_R$, where ω is the radian frequency, V_R is the Rayleigh wave velocity, $k = 2\pi/\lambda$ is the propagation constant, and λ is the wavelength.

Let the SAW signal at the plane z have an amplitude $A(z, w)$. In a linear system, $A(z, w)$ varies linearly with the amplitude of stress, strain, or particle velocity at any cross section of the plane z. Commonly, $|A(z, w)|$ is taken to be the square root of the power at the plane z. The elementary signal of frequency

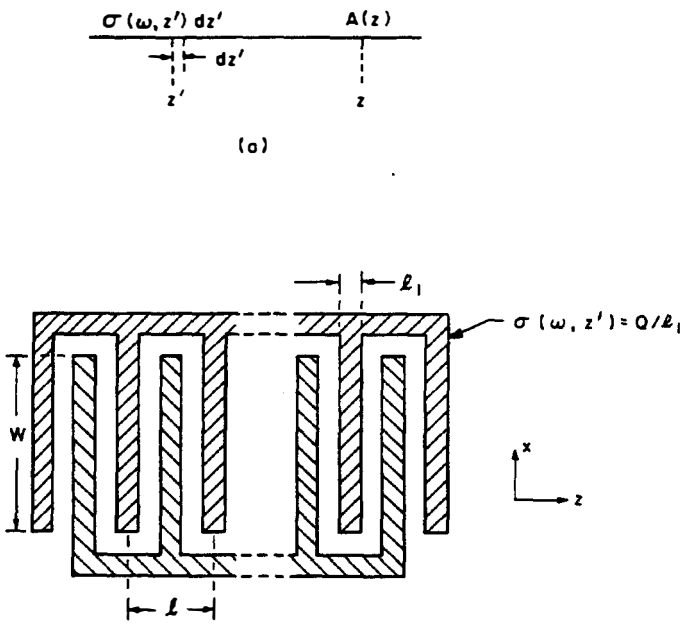

Figure 2.4.3 Notation used (a) to estimate the response of a transducer, and (b) for the finger pair spacing and width.

ω that reaches the plane z from the element between z' and $z' + dz'$ is of amplitude $dA(z, z', \omega)$. We can write

$$dA(z, z', \omega) = \alpha\sigma(\omega, z')\, e^{-jk(z-z')}\, dz' \tag{2.4.1}$$

where α is a coupling factor between the charge and the acoustic excitation and $k(z - z')$ is the phase shift of the wave between the excitation point z' and the observation point z. The signal amplitude $A(z)$ induced at z must be the sum of the contributions from all the elements of length dz' that are to the left of z. The total signal $A(z, \omega)$ reaching z is therefore

$$A(z, \omega) = \alpha \int_{-\infty}^{z} \sigma(\omega, z') e^{-jk(z-z')} dz' \tag{2.4.2}$$

If z is beyond the end of the exciting transducer, then $\sigma(z) = 0$, and we can write

$$A(z, \omega) = \alpha \int_{-\infty}^{\infty} \sigma(\omega, z')\, e^{-jk(z-z')} dz' \tag{2.4.3}$$

Thus *the output amplitude as a function of frequency is the Fourier transform of the charge on the fingers*. Since the frequency response of a transducer is the Fourier transform of its impulse response, it follows that the impulse response of a transducer is the same as the spatial charge distribution along its length. A different proof of this result based on time domain concepts is given in Sec. 4.2.

Example: Uniform Transducer

Consider the simple transducer with constant finger length and uniform finger pair spacing shown in Fig. 2.4.3. Suppose that the fingers have a *pair spacing* l and an individual width l_1, and that the charges on them are Q and $-Q$, in series.

We assume, for simplicity, that the charge is uniformly distributed on the fingers,† and that the amplitudes of all fields vary at a radian frequency ω. Hence, for a single finger (the right-hand one of a pair), we can write

$$\sigma = \frac{Q}{l_1} \tag{2.4.4}$$

If the center of this finger is at $z' = l/4$, its contribution to the field at the plane z is

$$\begin{aligned} A(z)\ [\text{single finger}] &= \frac{\alpha Q}{l_1} e^{-jk(z\ -\ l/4)} \int_{-l_1/2}^{l_1/2} e^{jkz'} dz' \\ &= \alpha Q e^{-jk(z\ -\ l/4)} \frac{\sin\ (kl_1/2)}{kl_1/2} \end{aligned} \tag{2.4.5}$$

The contribution of the left-hand finger of this pair, whose center is at $z' = -l/4$ and whose charge is $-Q$, can be added to this term to give

$$\begin{aligned} A(z)\ [\text{finger pair}] &= \alpha Q e^{-jkz} e^{jkl/4} - e^{-jkl/4} \frac{\sin\ (kl_1/2)}{kl_1/2} \\ &= 2\alpha j Q e^{-jkz} \sin \frac{kl}{4} \frac{\sin\ (kl_1/2)}{kl_1/2} \end{aligned} \tag{2.4.6}$$

We can now add the contributions from N finger pairs whose centers are at $z' = nl$ ($n = 0$ to $N - 1$), using the appropriate delays to obtain

$$\begin{aligned} A(z) &= 2j\alpha Q e^{-jkz} \sin \frac{kl}{4} \operatorname{sinc} \frac{l_1}{\lambda} \int_0^{N-1} e^{jknl} \\ &= 2j\alpha Q \sin \frac{kl}{4} e^{-jkz} \frac{\sin\ (kNl/2)}{\sin\ (kl/2)} \operatorname{sinc} \frac{l_1}{\lambda} e^{jk(N-1)l/2} \\ &= j\alpha Q e^{-jkz} \frac{\sin\ (kNl/2)}{\cos\ (kl/4)} \operatorname{sinc} \frac{l_1}{\lambda} e^{jk(N-1)l/2} \end{aligned} \tag{2.4.7}$$

where $\operatorname{sinc} x = \sin\ (\pi x)/(\pi x)$. Equation (2.4.7) is, of course, the Fourier transform of the charge distribution on the fingers. When N is large, the most rapidly varying function in Eq. (2.4.7) is the term $\sin\ (kNl/2)/\cos(kl/4)$. Using L'Hospital's rule, it can be shown that as $kl \to 2\pi$, this function has a peak value of $\pm 2N$ and is zero where

$$kl(\text{zero response}) = 2\pi\left(1 \pm \frac{1}{N}\right) \tag{2.4.8}$$

We conclude that as k is varied (the frequency is proportional to k, for $k = \omega/V_r$), the response is maximum where $kl = 2\pi$. Therefore, this value of k corresponds to the center frequency, or the *synchronous frequency*, $\omega = \omega_0$. At this point, $|A(z)| \to 2\alpha QN \operatorname{sinc}\ (l_1/l)$. It follows from Eq. (2.4.8) that the bandwidth between the zeros in the response is

$$\frac{(\Delta\omega)\ (\text{zeros})}{\omega_0} = \frac{2}{N} \tag{2.4.9}$$

†In practice the charge is peaked at the edges of the fingers: a single finger of width l_1 in free space has a charge distribution of the form $\rho_s = K/\sqrt{l_1^2/4 - x^2}$, where K is a constant. A more exact treatment of the problem uses a quasistatic solutions for a periodically spaced set of fingers.

If N is large, it is convenient to write

$$\frac{k - k_0}{} \quad \frac{\omega - \omega_0}{} \quad \frac{x}{} \tag{2.4.10}$$

In this case, it can be shown

$$\left|\frac{\sin}{x}\right. \tag{2.4.11}$$

where

$$\gamma = \alpha \operatorname{sinc} \frac{l_1}{\lambda} \tag{2.4.12}$$

and sinc (l_1/λ) is regarded as constant and of value sinc (l_1/l) over the bandwidth of th[illegible] is usually true. It [illegible] 2 is

$$\frac{}{} \quad \frac{}{} \tag{2.4.13}$$

Th[illegible] points where x [illegible] 4 dB.

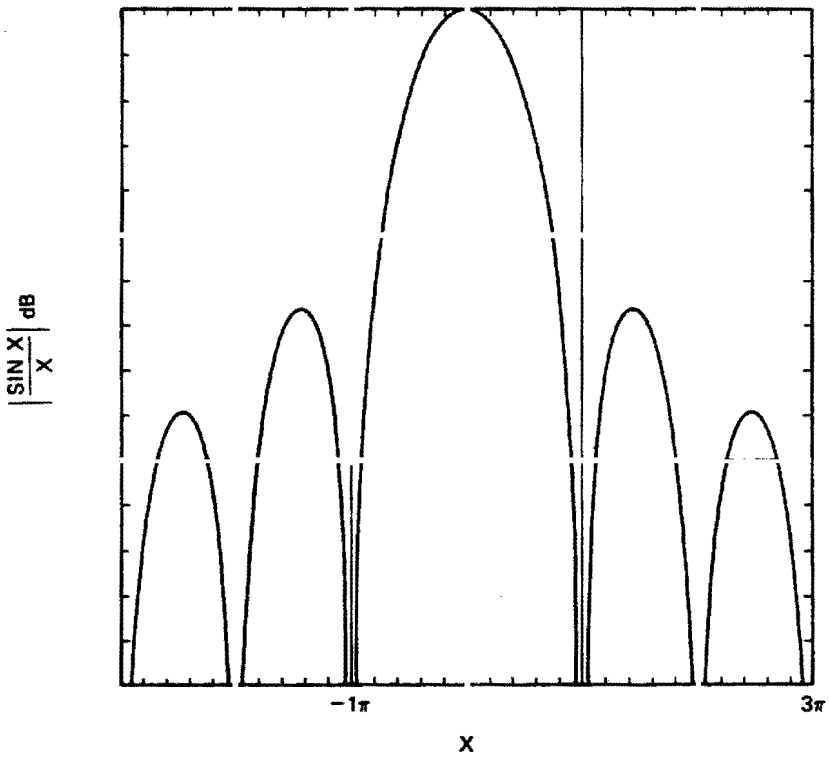

Figure 2.4.4 Plot of $|(\sin x)/x|$ as a function of x. (From Smith et al. [11].)

2.4.3 Network Theory of the Transducer

Several theories have been used to determine the electrical input impedance and frequency response of an interdigital transducer. The first, the *network theory*, is an equivalent-circuit method based on the idea that the response of a single finger pair is like that of a bulk wave transducer, so that the parameters of a single finger pair can be derived as if the finger pair were a bulk wave transducer (see Prob. 1.4.8). The N finger pairs are cascaded and connected together appropriately to establish the impedance matrix of the three-port network, comprised of the two acoustic ports, one at either end of the transducer, and the one electrical port.

A more fundamental approach to the theory is to use the *normal-mode formalism*, which is based on the conservation of power. While the equivalent-circuit method requires the use of empirically fitted parameters, this method allows us to obtain a solution for the electrical impedance of the transducer with no fitted parameters.

A third technique, developed by Ingebrigtsen [12], is based on wave impedance concepts. It, too, is useful and relatively simple; furthermore, it is often equivalent to, and sometimes more powerful than, normal-mode theory. But as it is a rather specialized method, we shall not deal with it here.

Another approach is a direct solution of the field theory [13]. This may be the most exact technique, but it is extremely complicated and inflexible and must be resolved for each new case. Generally, it is better to use a more physical theory, with some simplifying approximations, to get a physical understanding of what is happening in the system. The three approximate theories mentioned above have this advantage.

We shall first deal with the network theory, which was developed by Smith et al. [11]. They considered the system shown in Figs. 2.4.5 and 2.4.6(a), and based their theory of the transducer on the analogous one-dimensional models shown in Fig. 2.4.6(b) and (c). Following their method, we assume that a pair of bulk wave transducers is arranged acoustically in cascade and electrically in parallel so that the necessary electric field reversal takes place. For the configuration shown in Fig. 2.4.6(c), we assume that the component of applied electric field parallel to the direction of acoustic wave propagation is the most important. This is called the *in-line* model; it corresponds to a bulk wave transducer, of the type dealt with in Sec. 1.4, used with an equivalent circuit (the Mason equivalent circuit) of the type shown in Fig. 2.4.7, which we derived earlier (see Sec. 1.4.3). Alter-

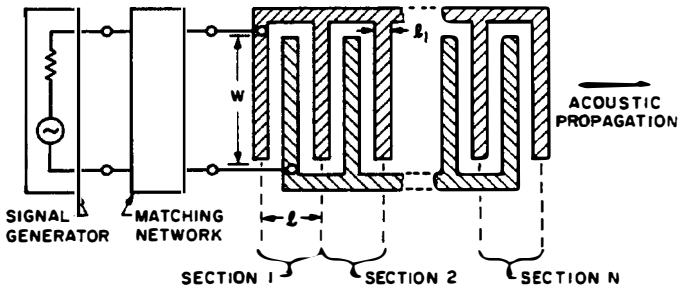

Figure 2.4.5 Interdigital transducer with its external circuit. (From Smith et al. [11].)

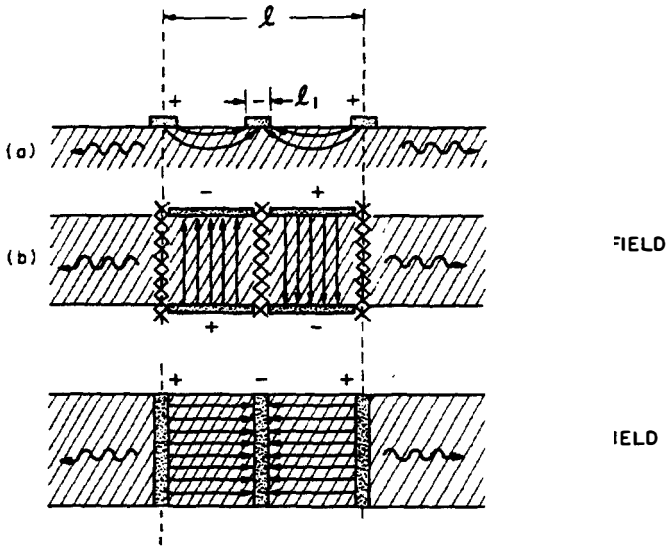

Figure 2.4.6 Side view of the interdigital transducer, showing field patterns: (a) actual field pattern; (b) crossed-field approximation; (c) in-line field approximation. (From Smith et al. [11].)

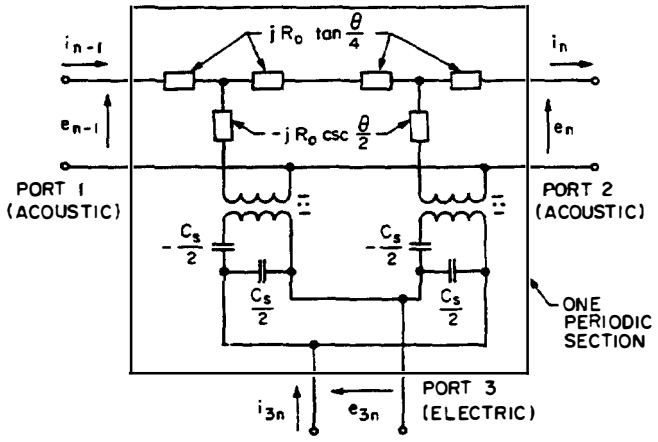

Figure 2.4.7 Mason equivalent circuit for one periodic section. The negative capacitors are short circuited for the crossed-field model: l, Periodic length; A, cross-sectional area; v, sound velocity; ρ, density; Z_0, $A\rho v$; h, piezo constant; f_0, v/L = synchronism frequency; θ, $2\pi(\omega/\omega_0)$ = periodic section transit angle; R_0, electrical equivalent of Z_0; C_s, electrode capacitance per section; K, electromechanical coupling constant. (From Smith et al. [11].)

natively, as shown in Fig. 2.4.6(b), we consider the field component normal to the surface to be the most important. We call this the *crossed-field* model; it is represented by the equivalent circuit shown in Fig. 2.4.7 (see Prob. 1.5.1). Its one difference from the in-line model is that it lacks a negative capacitor.

We define electrical equivalents to the acoustic force F_i and the terminal velocity V_i by setting

$$V_i = \frac{F_i}{\phi} \tag{2.4.14}$$

and

$$i_i = v_i \phi \tag{2.4.15}$$

where ϕ is the transformer ratio, defined as†

$$\phi = \frac{hC_s}{2} \tag{2.4.16}$$

† Note that here we use ϕ instead of N to avoid conflict with our definition for the number of finger pairs.

These definitions allow the mechanical impedance Z_0 of the substrate to be expressed in electrical ohms by the formula

$$R_0 = \frac{Z_0}{\phi^2} = \frac{2\pi}{\omega_0 C_s K^2} \tag{2.4.17}$$

where C_s is the capacitance of one periodic section and $\omega_0 = 2\pi f_0$ is the synchronous frequency defined by the formula $f_0 = V/l$, where l is the periodic length of the system, V is the acoustic velocity, and K is the effective electromechanical coupling constant for a surface acoustic wave.

The most difficult parameter to determine is the value of K, for the fields are no longer uniform within the transducer; thus an *effective* value of K is the best we can expect. Obviously, we cannot easily base our definition of K on the same type of field theory analysis used directly in the one-dimensional theory of the bulk wave transducer. It is possible to define K as the ratio of the stored electrical energy to the stored mechanical energy, but this definition is unreliable because in an interdigital transducer, not all the electric field lines intercept a single electrode pair, as they do in a bulk wave transducer.

A better definition is based on the velocity change of the wave in the medium when the RF field between the electrodes is shorted out, for it will give the same result, at least as far as the external electrical impedance is concerned, for bulk and SAW transducers. We know that the ratio of the stiffened to unstiffened velocity of a piezoelectric medium is $1+\Delta V/V = (1 + K^2)^{1/2}$. Therefore, the fractional change in velocity of a bulk wave transducer when the E field within the medium (i.e., between the electrodes) is made zero is

$$\frac{\Delta V}{V} = 1 - (1 + K^2)^{1/2} \approx \frac{-K^2}{2} \tag{2.4.18}$$

Now suppose that we place a metal film on the surface of the substrate. This is equivalent to shorting out the E field between the electrodes. In this case we measure a fractional change in velocity $\Delta V/V$. We then define the effective value of K on this basis, using Eq. (2.4.18). Thus we can relate the effective value of K to a parameter that can be experimentally measured or calculated from a field theory for the Rayleigh waves in a piezoelectric medium. This is a better procedure than the direct use of field theory for an interdigital transducer, because the boundary conditions are simpler.

In practice, we add a correction factor to Eq. (2.4.18) to compensate for the fact that this theory is heuristic, and for the effect of changing the finger width (the finger itself partially shorts out the fields). Thus, more generally, we write

$$K^2 = 2F \left| \frac{\Delta V}{V} \right| \tag{2.4.19}$$

where F is a "filling factor," which, as we discuss in Sec. 2.5 [see Eq. (2.5.43)], turns out to be about 1.12 when the strips and gaps between them are equal in size.

With the equivalent circuit for one periodic section given in Fig. 2.4.7, we can now calculate the admittance matrix for the connected N sections, as illustrated

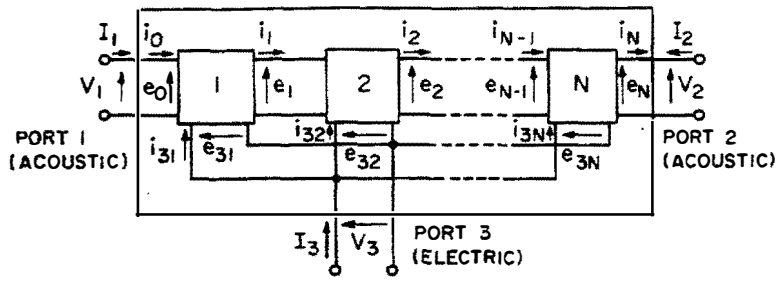

Figure 2.4.8 Transducer composed of N periodic sections, acoustically in cascade and electrically in parallel. (From Smith et al. [11].)

in Fig. 2.4.8. The three-port transducer equation is written like the equation for any three-port network, in the form

$$\begin{bmatrix} I_1 \\ I_2 \\ I_3 \end{bmatrix} = [Y] \begin{bmatrix} V_1 \\ V_2 \\ V_3 \end{bmatrix} \tag{2.4.20}$$

where the admittance matrix, because of the network's symmetry, can be written in the form

$$[Y] = \begin{bmatrix} Y_{11} & Y_{12} & Y_{13} \\ Y_{12} & -Y_{11} & -Y_{13} \\ Y_{13} & -Y_{13} & Y_{33} \end{bmatrix} \tag{2.4.21}$$

It is shown in Appendix F that for the crossed-field model, the admittances are

$$\begin{aligned} Y_{11} &= -jG_0 \cot N\theta \\ Y_{12} &= jG_0 \operatorname{cosec} N\theta \\ Y_{13} &= -jG_0 \tan \frac{\theta}{4} \\ Y_{33} &= j\omega C_T + 4jNG_0 \tan \frac{\theta}{4} \end{aligned} \tag{2.4.22}$$

For the in-line model, the admittances are

$$\begin{aligned} Y_{11} &= \frac{-S_{11}}{S_{12}} \\ Y_{12} &= \frac{1}{S_{12}} \\ Y_{13} &= \frac{-jG_0 \tan (\theta/4)}{1 - 2x \tan (\theta/4)} \\ Y_{33} &= \frac{j\omega C_T}{1 - 2x \tan (\theta/4)} \end{aligned} \tag{2.4.23}$$

where $G_0 = (R_0)^{-1}$, $C_T = NC_s$ is the capacity of the transducer, $\theta = 2\pi f/f_0 = kl$, and the matrix S is a complex function of N, θ, G_0, and C_s. Thus we have a complete three-port network model that can be used to calculate reflections from the transducer, its input admittance with different terminations, and so on.

The crossed-field model yields a simplified form of the admittance near synchronism. Writing $\theta = 2\pi + \delta$ and assuming that δ is small, we can show by the methods given in Appendix F that

$$[Y] = \frac{jG_0}{\delta}\begin{bmatrix} -\frac{1}{N} & \frac{1}{N} & 4 \\ \frac{1}{N} & -\frac{1}{N} & -4 \\ 4 & -4 & -16N + \frac{\delta\omega C_T}{G_0} \end{bmatrix} \tag{2.4.24}$$

Similar results for the synchronous case $\theta = 2\pi$ of the in-line model are given in Appendix F as Eq. (F.14).

We may determine the input impedance or admittance of the transducer by assuming that ports 1 and 3 are terminated with the matching admittance G_0. For the crossed-field model, the equivalent input circuit has the form

$$Y_3 = Y_a + j\omega C_T \tag{2.4.25}$$

where the acoustic contribution to the shunt admittance is given by the relation

$$Y_a = G_a(\omega) + jB_a(\omega) \tag{2.4.26}$$

where

$$G_a(\omega) = 2G_0\left(\tan\frac{\theta}{4}\sin\frac{N\theta}{2}\right)^2 \tag{2.4.27}$$

and

$$B_a(\omega) = G_0\tan\frac{\theta}{4}\left(4N + \tan\frac{\theta}{4}\sin N\theta\right) \tag{2.4.28}$$

as shown in Fig. 2.4.9(b).

For frequencies near synchronism, the resultant admittance can be stated in the simple forms, on which most design work is based, as follows:

$$G_a(\omega) = G_{a0}\left(\frac{\sin x}{x}\right)^2 \tag{2.4.29}$$

$$B_a(\omega) = G_{a0}\frac{\sin 2x - 2x}{2x^2} \tag{2.4.30}$$

where

$$x = \frac{N\pi(\omega - \omega_0)}{\omega_0} = \frac{N\delta}{2} \tag{2.4.31}$$

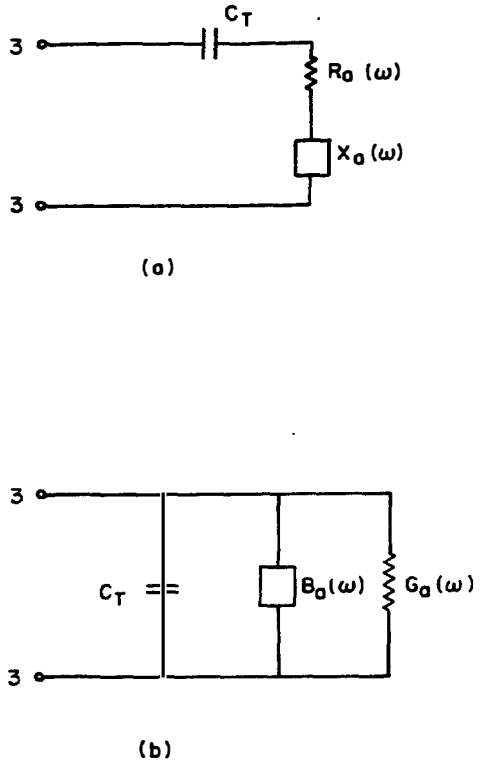

Figure 2.4.9 Transducer electrical input admittance: (a) series representation; (b) shunt representation.

and where

$$G_{a0} = \frac{4}{\pi} K^2 \omega_0 C_s N^2 F \tag{2.4.32}$$

is the synchronous conductance and $K^2 \approx 2|\Delta V/V|$.

Similar formulas can be obtained for the in-line circuit, which looks like a capacitance in series with the acoustic impedance. For this model, we write

$$Z_3 = Z_a + \frac{1}{j\omega C_T} \tag{2.4.33}$$

as illustrated in Fig. 2.4.9(a).

For frequencies near synchronism, we can now show that

$$Z_a = R_a + jX_a \tag{2.4.34}$$

with

$$R_a = R_{a0} \left(\frac{\sin x}{x}\right)^2 \left(\frac{\omega_0}{\omega}\right)^2 \tag{2.4.35}$$

and

$$X_a = X_{a0} \frac{}{2x^2} \left(\frac{}{\omega}\right)^2 \tag{2.4.36}$$

where

$$R_{a0} = \frac{4}{\pi}\frac{K^2F}{\omega_0 C_s} \tag{2.4.37}$$

where $K^2 = 2|\Delta V/V|$.

The series equivalent circuit predicts that the acoustic impedance Z_a is independent of N, although C_T is of course proportional to N. On the other hand, Y_a in the crossed-field model is proportional to N^2. Assuming that the capacitive reactance is much larger than the series impedance, we can show that the crossed-field result follows logically from the series formulation. We write

$$\begin{aligned} Y_3 \approx \frac{1}{Z_3} &\approx \frac{1}{Z_a + (1/j\omega C_T)} = \frac{Z_a - (1/j\omega C_T)}{Z_a^2 + (1/\omega^2 C_T^2)} \\ &\approx Z_a\omega^2 C_T^2 + j\omega C_T \end{aligned} \tag{2.4.38}$$

This result is identical to that which follows from Eqs. (2.4.25)–(2.4.32).

Using the crossed-field result, we see that the input radiation conductance G_a becomes zero at $x = \pi$, or where $(\omega - \omega_0)/\omega_0 = 1/N$. The acoustic Q, Q_a, is defined from the frequencies where the acoustic response is 3 dB down from the center frequency, that is,

$$Q_a = \frac{\omega_0}{\Delta\omega(3\text{ dB})} \tag{2.4.39}$$

where $\Delta\omega(3$ dB) is the frequency difference between the two -3-dB response points. However, it is more convenient to use the -4-dB points and ignore the slight error this yields because the resulting expression from the $(\sin x/x)$ function, taken where $x = \pi/2$, is so simple. We therefore write

$$Q_a \approx \frac{\omega_0}{\Delta\omega(4\text{ dB})} = N \tag{2.4.40}$$

Thus the larger the number of fingers, the higher the value of Q_a and the lower the bandwidth.

If we try to tune the transducer with a parallel inductance to eliminate the effect of the transducer capacity, the electrical Q, Q_e, will be

$$Q_e = \frac{\omega_0 C_T}{G_{a0}} = \frac{\pi}{4K^2NF} \tag{2.4.41}$$

When the number of fingers is smaller, Q_e increases because the capacity decreases. To obtain the lowest total Q, and hence the greatest bandwidth, we choose $Q_e = Q_a$. The condition for this to occur is

$$N^2 = \frac{\pi}{4K^2F} \tag{2.4.42}$$

Thus the maximum bandwidth is determined by the effective value of K. For lithium niobate, with an effective K^2 value of 0.046 and $F = 1.12$ [see discussion

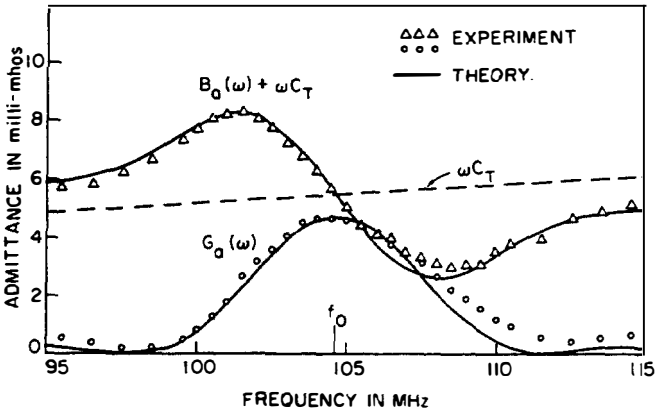

Figure 2.4.10 Measured radiation admittance for an $N = 15$ transducer on YZ lithium niobate, compared with theoretical curves calculated from the crossed-field model. (After Smith et al. [11].)

after Eq. (2.5.42)], the optimum number of fingers is 4 and the bandwidth is of the order of 20%.

A similar treatment for the in-line model gives the same result. Experiments confirm the theoretical results very accurately. An early experimental result is compared to theory in Fig. 2.4.10. This network theory has been widely used in the design of transducers and, in practice, provides accurate, comprehensible results.

PROBLEM SET 2.4

1. The assumption that the charge on the interdigital fingers is uniform is a crude approximation. It is better to write

$$\sigma = \sigma_0 l_1 \left(\frac{l_1^2}{4 - z^2}\right)^{-1/2}$$

for each finger.

(a) Find σ_0 in terms of Q. Find $A(Z,\omega)$ for an N-finger pair with a period l.

Hint. Put $z = (l_1/2) \sin \theta$ and use the Bessel function formula

$$J_0(x) = \frac{1}{\pi} \int_0^{\pi} e^{jx \sin \theta} \, d\theta$$

(b) Consider an interdigital transducer for which $l_1 = l/4$. What is the ratio of the excitation amplitude to the total charge at the center frequency? Compare your result to that obtained with the use of the uniform charge assumption.

2. A transducer uses three fingers for each section, as illustrated below. These three fingers are supplied by a three-phase system, with signals exp $[j(\omega t - \pi/3)]$, $-\exp(j\omega t)$, and exp $[j(\omega t + \pi/3)]$. The most convenient way to obtain a three-phase excitation is to connect one set of electrodes to ground, to make the voltage between the input grounded electrode and the input terminals exp $(j\omega t - \pi/3)$.

Work out the excitation of waves in the forward and backward directions, respectively. Take the fingers to have a width l_1 and the period of the transducer to be l.

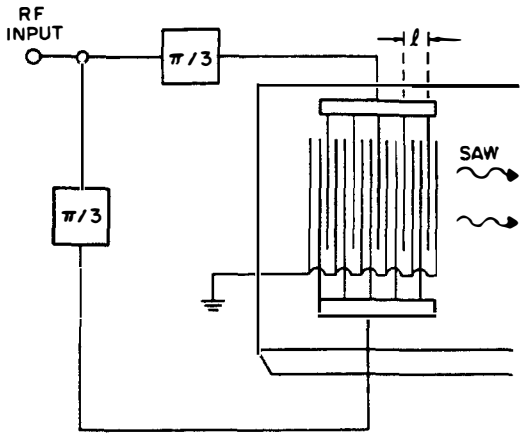

Assume that $l_1 << l$, that the charges on the fingers are of magnitude Q, and that the charge density is uniform on each finger.

3. **(a)** Consider the network circuit theory of an interdigital transducer. Use the KLM model, as illustrated in Fig. 1.4.12, to write down a circuit for the in-line field model that is equivalent to the one obtained using the Mason model, as illustrated in Fig. 2.4.7. Do not work out the theory of this transducer.
   (b) How would you modify the circuit to take account of a finite finger width l_1? The region under the finger can be regarded as a transmission line of slightly different impedance from the region between the fingers (the gap).
4. Prove Eqs. (2.4.29) and (2.4.30) from Eqs. (2.4.27) and (2.4.28).

2.5 NORMAL-MODE THEORY AND PERTURBATION THEORY

2.5.1 Introduction

The problem of determining the excitation of surface acoustic waves or other types of waveguide modes by a transducer is difficult to tackle directly. In the same way, it is difficult to determine the effects of small perturbations of the medium directly. For instance, if a metal strip is placed on the surface of the medium on which a surface acoustic wave is propagating, the wave will be perturbed. Generally, part of the wave will be reflected by the obstruction, part transmitted past it, and part may be converted to a bulk shear or longitudinal wave.

Problems of this type can sometimes be solved exactly by carrying out a detailed field theory analysis and taking account of the boundary conditions at the perturbation. But as discussed in Sec. 2.4.3, it is extremely difficult to apply such techniques, except in the simplest cases, because it is hard to satisfy the boundary conditions for all the field components of interest. Even when the exact field theory can be solved, it tends to be extremely complicated in mathematical form and provides very little intuition about the basic parameters governing the solution. Furthermore, again as mentioned in Sec. 2.4.3, field theories must be solved anew for each individual case.

For example, when a thin metal film a fraction of a wavelength in thickness is evaporated onto a substrate, the solution for the surface acoustic wave must obviously be very close to the solution for the original unperturbed substrate. But to determine the perturbation by an exact field theory would mean solving the problem again completely. Instead, however, we can find the required solution by using a perturbation theory, which will provide more physical insight into the solution. Field theory is an even less desirable choice when a thin film covers only a short region of the substrate, for the solution then becomes so complicated that we tend to lose physical insight into the problem.

Here we discuss a perturbation theory based on the idea that the total field in a perturbed medium is very similar to a field of a wave in the unperturbed medium. In Appendix E, this theoretical approach is justified on a more rigorous basis by expressing the total field of a single mode in the perturbed medium as a weighted sum of the original modes in the unperturbed medium. When the perturbation is small, only one of these unperturbed modes is strongly excited.

This mode expansion technique is similar to Fourier analysis or, more generally, the expansion of a function in terms of a sum of orthogonal functions. For instance, if $F(x)$ is a periodic function with a period 2π, we can write

$$F(x) = \sum_n A_n e^{jnx} \tag{2.5.1}$$

and use the orthogonality relation

$$\frac{1}{2\pi}\int_0^{2\pi} e^{j(m-n)x}\,dx = \delta_{nm} \tag{2.5.2}$$

where $\delta_{nm} = 1$ when $n = m$ and $\delta_{nm} = 0$ when $n \neq m$, to show that

$$A_n = \frac{1}{2\pi}\int_0^{2\pi} F(x)e^{-jnx}\,dx \tag{2.5.3}$$

If $F(x)$ is a function very close in form to $\exp(jNx)$, the dominant term in the expression of Eq. (2.5.1) is that for $n = N$. This analogy holds exactly for rectangular electromagnetic waveguides, where any arbitrary cross-sectional variation of the field in the waveguide can be expressed as the sum of a set of trigonometric functions (the wave solutions for the individual modes of the waveguide). More generally, however, the same kinds of analogies still hold, and we can work in terms of the wave solutions of the unperturbed system to determine the nature of the waves in the perturbed system.

One advantage of this method is it allows us to find the amplitude of a mode that is excited in a waveguide without detailed knowledge of the fields in the exciting region. For instance, we need only a relatively crude estimate of the charge distribution on the metal electrodes of an interdigital transducer to determine the amplitudes of the excited waves and the transducer input impedance. Here we use the procedure of Sec. 2.4.2 to obtain quantitative results.

We state the amplitude of an excited wave in terms of the power flow associated with it. Because power flow is a one-dimensional concept, the final results

are often very simple in form and provide a great deal of physical insight into the interactions involved. The concept is particularly useful for dealing with piezoelectric materials because power has a meaning for both electromagnetic and acoustic fields. Thus, to determine how a piezoelectric transducer is excited by a surface acoustic wave, it is useful to be able to work in terms of power concepts. [9].

2.5.2 Power Flow Concepts

Before beginning a detailed analysis for the excitation of a surface acoustic wave, we must express the surface acoustic wave (SAW) amplitude in terms of the power flow. Suppose that the amplitude of any component of the wave is $A(z)$. In general, if the amplitude is associated with stress, strain, velocity, or some other component of the wave, it has a fixed cross-sectional variation. The power in the wave, however, varies as the square of the amplitude. Thus it is convenient to choose the amplitude $A(z)$ to be directly associated with the total power of the wave, which is a one-dimensional parameter [9, 15]. We call the power of the wave $A(z)$ propagating in the forward direction P_F, and define it as

$$P_F = AA^* \tag{2.5.4}$$

We use an amplitude parameter $B(z)$ for a wave propagating in the backward direction and take the power P_B associated with it to be

$$P_B = -BB^* \tag{2.5.5}$$

We can connect this concept with the stress and strain components in a general way because the stress, strain, velocity, and displacement vary linearly in amplitude with $A(z)$. Thus if we know $A(z)$, in principle we also know the amplitude of the stress at any point $\mathbf{T}(x, y, z)$ and the amplitudes of all the other field components.

We shall find it convenient to express the cross-sectional variations of the fields in a normalized form so that they correspond to unit power flow in the guide. When the nth mode is excited by the fields at a perturbation, its amplitude does not necessarily vary as $\exp(-jk_nz)$. Thus for the nth mode with a propagation constant k_n, we more generally write

$$\hat{v}_n(x,y,z) = A_n(z)\mathbf{v}_n(x, y) \tag{2.5.6}$$

$$\hat{\mathbf{T}}_n(x,y,z) = A_n(z)\mathbf{T}_n(x,y) \tag{2.5.7}$$

$$\hat{\phi}_n(x,y,z) = A_n(z)\phi_n(x, y) \tag{2.5.8}$$

and

$$\hat{\mathbf{D}}_n(x,y,z) = A_n(z)\mathbf{D}_n(x,y) \tag{2.5.9}$$

where $\hat{\phi}_n$ is the electric potential and $\mathbf{T}_n(x, y)$, $\mathbf{v}_n(x, y)$, $\phi_n(x, y)$, and $\mathbf{D}_n(x, y)$ are the cross-sectional variations of the components of the nth mode. The symbol is associated with the field variation in the z direction. For an unperturbed mode (i.e., a mode in the unperturbed guide), $A_n(z) = \exp(-jk_nz)$.

The power flow P_n associated with this propagating wave is the sum of the electromagnetic and acoustic power flows (see Sec. 1.2 and Appendix E), where [4, 9]

$$P_n = \frac{1}{2}\,\mathrm{Re}\left(A_n A_n^* \int_s (\mathbf{E}_n^* \times \mathbf{H}_n - \mathbf{v}_n^* \cdot \mathbf{T}_n)\mathbf{a}_z\, ds\right) \tag{2.5.10}$$

The phase velocity of a surface acoustic wave is typically several orders of magnitude less than that of light. This means that we can neglect RF magnetic fields, put $\nabla \times \mathbf{E} = 0$, and write the electric field in terms of a quasistatic electric potential ϕ, with $\mathbf{E} = -\nabla\phi$. In this case (see Prob. 1),

$$P_n = \frac{1}{2}\,\mathrm{Re}\left(A_n A_n^* \int_s (j\omega \mathbf{D}_n \phi_n^* - \mathbf{v}_n^* \cdot \mathbf{T}_n) \cdot \mathbf{a}_z\, ds\right) \tag{2.5.11}$$

where $j\omega\mathbf{D}_n \cdot \mathbf{a}_z$ is the displacement current density in the z direction and s is the cross-sectional area of the system.

Normalization. We choose the amplitudes of the normalized fields $\mathbf{v}_n$, $\mathbf{T}_n$, ϕ_n, and $\mathbf{D}_n$, so that for a propagating wave,

$$\frac{1}{2}\,\mathrm{Re}\int_s (j\omega \mathbf{D}_n \phi_n^* - \mathbf{v}_n^* \cdot \mathbf{T}_n) \cdot \mathbf{a}_z\, ds = \pm 1 \tag{2.5.12}$$

where the $+$ and $-$ signs denote waves propagating in the forward $(+z)$ and backward $(-z)$ directions, respectively. Thus we have chosen the amplitudes of the normalized fields $\mathbf{v}_n$, $\mathbf{T}_n$, ϕ_n, and $\mathbf{D}_n$ to correspond to unit power flow. In this case, it follows that the power flow P_{Fn} associated with the nth forward wave mode is

$$P_{Fn} = A_n A_n^* \tag{2.5.13}$$

while that associated with the nth backward wave mode, P_{Bn}, is

$$P_{Bn} = -A_{-n} A_{-n}^* = -B_n B_n^* \tag{2.5.14}$$

We have used the symbol B_n, rather than A_{-n}, to indicate the nth backward wave mode. Therefore, the total real power flow P_n in the nth forward and backward modes is

$$P_n = A_n A_n^* - B_n B_n^* \tag{2.5.15}$$

2.5.3 Excitation of a Surface Acoustic Wave

Here we give a heuristic derivation of the perturbation theory for the excitation of the nth mode. A more rigorous derivation of the results, using mode orthogonality, is given in Appendix E.

Suppose that the nth forward wave mode is excited from an external source of amplitude $f(z')\,dz'$ in an element of length dz'. Typical examples are the charges on a set of electrodes, which couple from another acoustic beam or scatter

from an inhomogeneity. As we have already seen in Sec. 2.5.2, because the system is linear and the guide is taken to be uniform, the signal reaching the plane z must be of the form

$$dA_n(z) = \alpha_n f(z')e^{-jk_n(z-z')}\,dz' \tag{2.5.16}$$

where we have used the subscript n to denote the nth mode and α_n is a coupling parameter from the external source to the nth mode. If $f(z')$ is doubled in amplitude, so is $A(z)$, as it should be in a linear system. If there is a distributed excitation, we can write the *excitation equation* in the following integral form:

$$A_n(z) = \alpha_n \int_{-\infty}^{z} f(z')\, e^{-jk_n(z-z')}\,dz' = \int_{-\infty}^{z} g_n(z')e^{-jk_n(z-z')}\,dz' \tag{2.5.17}$$

where now we have combined $\alpha_n f(z')$ into one parameter, $g_n(z')$.

By taking the exp $(-jk_nz)$ term outside the integral, Eq. (2.5.17) may be differentiated with respect to z to obtain the differential form of the *excitation equation*:

$$\frac{dA_n}{dz} + jk_nA_n = g_n(z) = \alpha_n f(z) \tag{2.5.18}$$

Equations (2.5.17) and (2.5.18) imply that if we know the excitation as a function of z and can determine the coupling coefficient α or the parameter $g_n(z)$, we can determine the amplitude $A_n(z)$ and hence the power of the wave excited at any plane z. Outside the excitation region $[g_n(z) = 0]$, the solution is of the form $A_n(z) \sim \exp(-jk_nz)$. A similar derivation can be carried out for the backward wave or other modes of the system.

Physical implications of the excitation equations. Using the simple form of Eq. (2.5.18), we can usually determine how the distribution of the excitation will affect the amplitude of the final wave, even without a quantitative knowledge of α_n.

Suppose that the excitation is of the form $f(z') = f_0(z')\exp(-j\beta z')$ and $\beta \neq k$. From Eq. (2.5.17) or Eq. (2.5.18), if $f(z')$ is finite over a region many wavelengths long, the net excitation of the surface acoustic wave of amplitude $A_n(z)$ tends to be small, because if $\beta \neq k$, the waves excited at planes $z' < z$ arrive at the plane z out of phase.

Now suppose that $f_0(z')$ is constant from $z' = 0$ to $z' = L$, and that $\beta = k_n$. The excitation is then cumulative at the plane z, so that $A_n(L) = \alpha_n f_0 L$ and $A_n(L)$ increases linearly with L. Thus, even without knowing the coupling coefficient α_n, we can gather much information about the nature of the excitation.

Quantitative evaluation of $g_n(z)$. We can derive the value of $g_n(z)$ in terms of the exciting fields at the surface of a SAW waveguide by regarding these fields as perturbations at the waveguide surface that change the power flow along the guide. Let us consider a piezoelectric waveguide, as illustrated in Fig. 2.5.1,

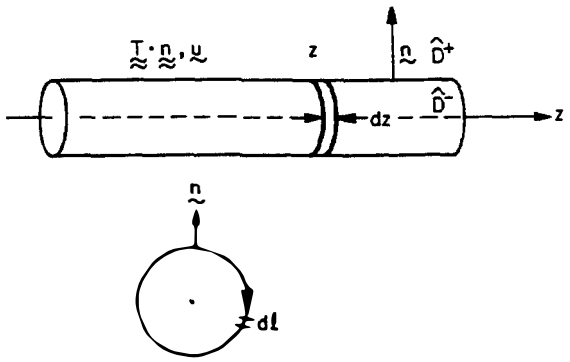

Figure 2.5.1 Notation used in the normal mode theory for a cylindrical system that is uniform in the z direction. The shape of the guide is arbitrary.

for which the boundary conditions for the nth mode are such that the normal stress is zero, that is

$$\mathbf{T}_n \cdot \mathbf{n} = 0 \tag{2.5.19}$$

and there is no surface charge, that is, the boundary condition on the normal electric displacement densities of the nth mode $\mathbf{D}_n$ is

$$(\mathbf{D}_n^+ - \mathbf{D}_n^-) \cdot \mathbf{n} = 0 \tag{2.5.20}$$

where $\mathbf{D}_n^+$ and $\mathbf{D}_n^-$ are the electric displacement densities just outside and just inside the surface, respectively, and $\mathbf{n}$ is the outward unit vector normal to the surface.

We derive the excitation parameter $g_n(z)$ by assuming that there is a finite normal stress $\hat{\mathbf{T}} \cdot \mathbf{n}$ and surface charge $\hat{\rho}_s$ at the boundary surface of the guide. Thus the boundary conditions for an unperturbed mode are no longer satisfied. The required derivation is carried out rigorously in Appendix E. Here we will carry out the derivation heuristically by using the concept of conservation of real power.

The velocity due to the nth mode at the surface of the guide is $A_n v_n(x, y)$, while the potential is $A_n \phi_n(x, y)$. Therefore, the power delivered to the nth mode by an outward normal applied stress $\hat{\mathbf{T}} \cdot \mathbf{n}$ and an electric surface charge density $\hat{\rho}_s = (\hat{\mathbf{D}}^+ - \hat{\mathbf{D}}^-) \cdot \mathbf{n}$ is $\frac{1}{2}\,\mathrm{Re}\,[j\omega\hat{\rho}_s\phi_n^* + \hat{\mathbf{T}} \cdot \mathbf{v}_n^*]A_n^*$. Here the + and − superscripts are associated with the fields just outside and just inside the surface, respectively. Thus the rate of change of real power in the nth forward mode is

$$\frac{dP_n}{dz} = \frac{d}{dz}(A_n A_n^*) = \tfrac{1}{2}\int_l \mathbf{A}_n^* \left[(\hat{\mathbf{T}} \cdot \mathbf{v}_n^*) \cdot \mathbf{n} + j\omega\hat{\rho}_s\phi_n^*\right] dl \tag{2.5.21}$$

where the integral is taken around the periphery of the guide at a plane z and the displacement current per unit area flowing into the guide is $j\omega\rho_s$.

Multiplying Eq. (2.5.18) by A_n^* and adding the result to its complex conjugate, we can show that

$$A_n^* \frac{dA_n}{dz} + A_n \frac{dA_n^*}{dz} = A_n^* g_n + A_n g_n^* \tag{2.5.22}$$

This relation can be written in the form

$$\frac{d}{dz}(A_n A_n^*) = 2(\mathbf{A}_n^* g_n) \tag{2.5.23}$$

Comparing this expression with Eq. (2.5.21), we can write

$$g_n(z) = \tfrac{1}{4}\int_l [(\hat{\mathbf{T}} \cdot \mathbf{v}_n^*) \cdot \mathbf{n} + j\omega\hat{\rho}_s\phi_n^*]\, dl \tag{2.5.24}$$

Thus

$$\frac{dA_n}{dz} + jk_nA_n = \tfrac{1}{4}\int_l [(\hat{\mathbf{T}} \cdot \mathbf{v}_n^*) \cdot \mathbf{n} + j\omega\hat{\rho}_s\phi_n^*]\, dl \tag{2.5.25}$$

This is the relation required for the excitation of the nth mode of the system.

2.5.4 Perturbation Theory of the Interdigital Transducer

We now use the results of Secs. 2.5.2 and 2.5.3 to determine how surface acoustic waves are excited by an interdigital transducer extending from $z = 0$ to $z = L$. We derive the input impedance of the transducer, dropping the use of the subscript n, as we are interested only in the surface acoustic wave mode, and finding the amplitude of the forward wave $A(z)$ at points $z > L$ and of the backward wave $B(z)$ at points $z < 0$. Because of symmetry, we expect that $|A(L)| = |B(0)|$. Thus when a transducer converts an electrical signal to an acoustic wave traveling in one direction, and vice versa, there will be a 3-dB loss.

We determine the input impedance of the transducer by finding the total acoustic power P excited by the transducer. Because of conservation of power [Poynting's theorem; Eq. (1.3.2)], we can define the electrical input resistance R_a of the transducer as

$$R_a = \frac{2P}{II^*} \tag{2.5.26}$$

where I is the current into the transducer. We must now derive A more quantitatively than in Sec. 2.5.2.

Consider the piezoelectric substrate, illustrated in Fig. 2.5.2, in which waves are excited by metal electrodes or by charges in a semiconductor. Initially, we suppose that there is a charge per unit length $\sigma(z') = \rho_s(z')w$ at any point along the substrate within the acoustic beam width w, where the charge per unit area $P_s(z')$ is assumed to be uniform over a width w. From Eq. (2.5.25),

$$\frac{dA}{dz} + jkA = \frac{j\omega}{4}\sigma\phi_0^* \tag{2.5.27}$$

where we have used the subscript 0 to indicate that ϕ_n is associated with the principal mode, and have dropped the subscript n on A and k.

We may treat the excitation of the backward traveling wave in a similar way, writing

$$\frac{dB}{dz} - jkB = -\frac{j\omega}{4}\sigma\phi_0^* \tag{2.5.28}$$

where B denotes the wave traveling in the backward direction, as discussed in

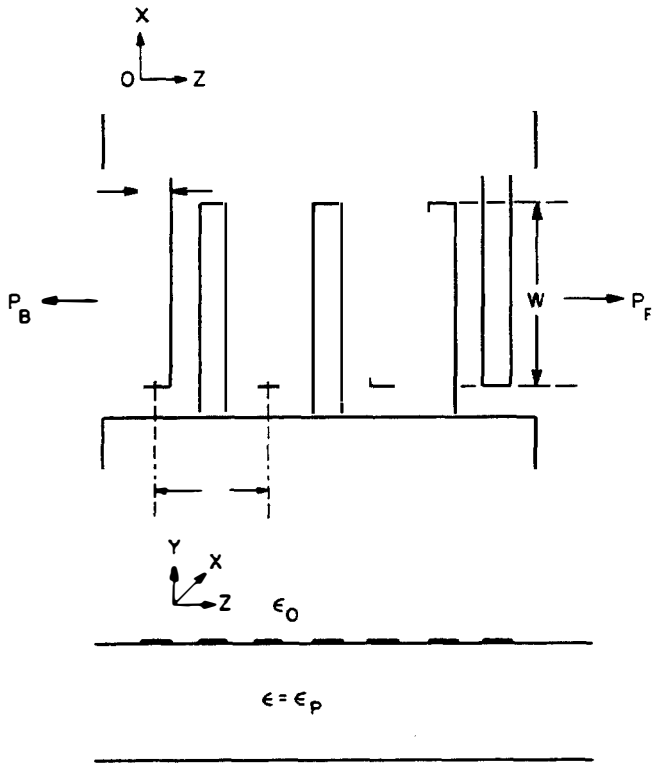

Figure 2.5.2 Interdigital transducer.

Appendix E, and we take $\phi_0 = -\phi_{-0}$ and $P_{-0} = -P_0$. When there is no excitation [$\sigma(z) = 0$], the solutions of Eqs. (2.5.27) and (2.5.28) vary as exp $(-jkz)$ and exp (jkz), respectively.

Now we can use Eqs. (2.5.27) and (2.5.28) to determine the input impedance of the interdigital transducer as a function of frequency. We will not do this in the most general way, but will instead determine only the real part of the input impedance of the interdigital transducer. From this result, we can determine the reactive part of the input impedance by using a Hilbert transform [15, 16]. The result is equivalent to the series in-line model of the circuit theory, which was described in Sec. 2.4.3. Following very similar procedures, a result equivalent to that of the crossed-field model can be obtained. The reader is referred to the paper by Auld and Kino [9] for further details of the full theory.

Suppose that we consider an interdigital structure with N finger pairs, each finger of length w, and width l_1; the periodic length is l and the transducer extends from $z = 0$ to L for a total length L. We can assume that the surface charge $\sigma(z)$ on each finger is uniform and of value Q/l_1. A schematic of this system is shown in Fig. 2.5.2.

We use Eq. (2.5.27) to replace α in Eqs. (2.4.3), (2.4.7), and (2.5.18) and write

$$\alpha = \frac{j\omega\phi_0^*}{4} \tag{2.5.29}$$

From Eq. (2.4.7),

$$|A(L)| = \frac{\omega\phi_0^* Q}{4} \left| \frac{\sin(Nkl/2)}{\cos(kl/4)} \frac{\sin(kl_1/2)}{kl_1/2} \right| \tag{2.5.30}$$

Similarly,

$$|B(0)| = \frac{\omega\phi_0^* Q}{4} \left| \frac{\sin(Nkl/2)}{\cos(kl/4)} \frac{\sin(kl_1/2)}{(kl_1/2)} \right| \tag{2.5.31}$$

The total electrical power input to the transducer is

$$P = |A(L)|^2 + |B(0)|^2 \tag{2.5.32}$$

The input current to the transducer is

$$I = j\omega NQ \tag{2.5.33}$$

We have defined the electrical radiation resistance R_a of the transducer as

$$R_a = \frac{2P}{II^*} \tag{2.5.34}$$

Substituting Eqs. (2.5.30)–(2.5.33) into Eq. (2.5.34) results in

$$R_a = \frac{Z_0}{2} \left(\frac{\sin(Nkl/2)}{N\cos(kl/4)} \frac{\sin(kl_1/2)}{(kl_1/2)} \right)^2 \tag{2.5.35}$$

where we define the wave impedance Z_0 as the

$$Z_0 = \frac{\phi_0 \phi_0^*}{2} \tag{2.5.36}$$

The normalized potential ϕ_0, and hence the wave impedance Z_0, can be evaluated directly from the exact field theory for a Rayleigh wave propagating on the unperturbed substrate.

We can also evaluate the impedance Z_0 another way. First we use the field theory to solve a simpler problem, determining the propagation constant of a surface acoustic wave on a piezoelectric substrate with a uniform perfect conductor deposited on it. Then we solve the same problem by perturbation theory and compare the two results.

As an example, we can begin by finding the change in velocity when an infinitesimally thin metal conductor is deposited on the piezoelectric substrate. This problem can be solved by field theory. In this case, the potential ϕ at the surface is forced to become zero, which changes the propagation constant from k to k' and the wave velocity from V to $V + \Delta V$. As we might expect, $|\Delta V/V|$ is directly proportional to the coupling coefficient α_0 or impedance Z_0, for if the electrical coupling is zero, an infinitesimally thin metal conductor cannot interact with the wave. On the other hand, if the value of $|\Delta V/V|$ is large, the potential at the surface for a given power flow is large, as is the interaction with charges at

the surface. Thus we can work in terms of the coupling coefficient α, the relative change in velocity $\Delta V/V$, or the impedance of the wave at the surface defined as $Z_0 = \Phi_0^2/2P_0 = \phi_0^2/2$, where Φ_0 is the unnormalized potential at the surface for a wave traveling on the free piezoelectric substrate and P_0 is the total power in the wave.

Appendix D shows that

$$Z_0 = \frac{2}{\omega(\varepsilon + \varepsilon_0)w} \left|\frac{\Delta V}{V}\right| \tag{2.5.37}$$

where ε is the permittivity of the medium. Thus

$$R_a = \frac{1}{\omega(\varepsilon_0 + \varepsilon)w} \left(\frac{\sin (Nkl/2)}{N \cos (kl/4)} \frac{\sin (kl_1/2)}{kl_1/2}\right)^2 \left|\frac{\Delta V}{V}\right| \tag{2.5.38}$$

We now consider the frequency response of the transducer. We assume that it is operated near the synchronous frequency $\omega = \omega_0$, so that $kl \approx 2\pi$ and $kl_1 \approx 2\pi l_1/l$. Putting $x = N\pi(\omega - \omega_0)/\omega_0$ in Eq. (2.5.38), we find that if N is large, the input resistance R_a may be written in the approximate form

$$R_a \approx \frac{\omega_0}{\omega} R_{a0} \left(\frac{\sin x}{x}\right)^2 \tag{2.5.39}$$

where

$$R_{a0} = \frac{4}{\omega_0(\varepsilon_0 + \varepsilon)w} \left(\frac{\sin (\pi l_1/l)}{(\pi l_1/l)}\right)^2 \left|\frac{\Delta V}{V}\right| \tag{2.5.40}$$

When $l_1 = l/4$ (equal strip and gap widths), R_{a0} becomes

$$R_{a0} = \frac{32}{\pi^2\omega_0 (\varepsilon_0 + \varepsilon)w} \left|\frac{\Delta V}{V}\right| \tag{2.5.41}$$

We may compare this result to Eq. (2.4.37), obtained from the circuit theory of Sec. 2.4.3. Equation (2.4.37) has a very similar frequency dependence and a value of R_{a0} corresponding to

$$R_{a0} = \frac{8}{\pi} \frac{F}{\omega_0 C_s} \left|\frac{\Delta V}{V}\right| \tag{2.5.42}$$

where C_s is the capacity per finger pair. From electrostatic theory, if $l_1 = l/4$ (equal strip width and spacing), then $C_s = w(\varepsilon_0 + \varepsilon)$. Equation (2.5.41) yields a numerical factor, $32/\pi^2 = 3.24$; the circuit theory for an interdigital transducer gives a factor $8F/\pi$, or $2.54F$.

A more accurate derivation of the perturbation theory, based on the true electrostatic distribution of the charge on the fingers, with $l_1 = l/4$ [27], leads to the result

$$R_{a0} = \frac{2.87}{\omega_0 C_s} \left|\frac{\Delta V}{V}\right| \tag{2.5.43}$$

We conclude that the parameter F must have a value of $2.87/2.54 = 1.12$.

One more change is needed to make this model conform to reality. We must take the permittivity of a piezoelectric material to be anisotropic. This is done easily; we need only replace ε by a parameter ε_p, defined by the relation

$$\varepsilon_p = (\varepsilon_{yy}\varepsilon_{zz} - \varepsilon_{yz}^2)^{1/2} \tag{2.5.44}$$

Careful comparisons have been made between this normal mode theory and the experimental results for R_{a0} taken on Y-cut lithium niobate with propagation in the z direction and with $\varepsilon_p = 50\varepsilon_0$, which corresponds to the stress-free values of the dielectric constant ε_{ij}^T. When the value of $|\Delta V/V|$ is taken to be 0.023, the experimental and theoretical results agree to within less than 1%.

Note that here we have neither calculated the transducer capacity directly nor shown its connection with the acoustic theory. In Appendix D, however, we derive the *electrostatic field*, which results from the charge. Similarly, when there is a charge on the electrodes of the transducer, we must determine the two potentials resulting from it: the acoustic potential ϕ_a, which we determine from the perturbation theory and the electrostatic potential. The electrostatic potential is, of course, associated with the capacity of the transducer; it gives an additional potential in series with the acoustic term and hence a capacity in series with the acoustic impedance. This capacity C_T is calculable by methods very similar to those given above, or by a direct solution of electrostatic theory, as

$$C_T = N\varepsilon_p w \tag{2.5.45}$$

where $l_1 = l/4$.

2.5.5 Leaky Waves

Now consider the effect on a surface acoustic wave when the surface of the substrate on which it propagates is loaded by another semi-infinite medium such as air or water. We assume that a wave can propagate in this medium with a phase velocity lower than that of the surface acoustic wave on the free substrate. If a surface acoustic wave with a propagation constant β is then excited on the substrate, we expect it to excite a quasi-plane wave in the liquid propagating at an angle θ to the normal, as illustrated in Fig. 2.5.3, with

$$k \sin\theta = \beta \tag{2.5.46}$$

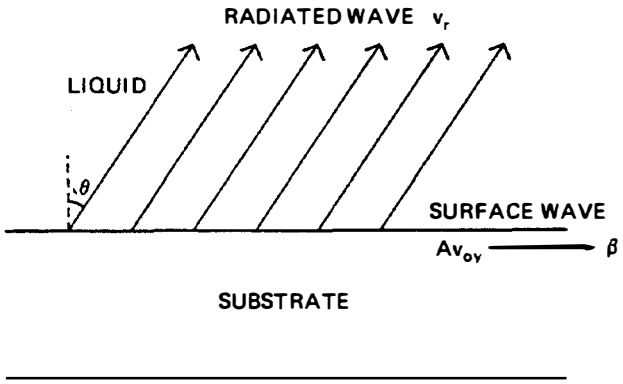

Figure 2.5.3 Leaky surface wave radiating into a liquid or into another medium that propagates a wave with a lower phase velocity than the surface wave.

or

$$V_R \sin \theta = V_L \tag{2.5.47}$$

where k is the propagation constant in the liquid. To avoid confusion, we have changed the notation for the propagation constant on the substrate. The wave velocity in the liquid is now V_L, and V_R is the Rayleigh wave phase velocity. Thus, under these conditions, power is continuously radiated into the liquid medium and the surface acoustic wave is attenuated so that its propagation constant changes from β to $\beta - j\alpha$ (i.e., the wave amplitude varies as $\exp[-(j\beta + \alpha)z]$). Such a wave is known as a *leaky wave*. In principle, it can exist as a simple outgoing wave only if the upper medium is semi-infinite. When the upper medium is finite in extent, it forms a type of waveguide and the radiated wave is reflected from the top surface of the medium. Thus energy is not radiated, although there may be several propagating modes in the liquid waveguide into which the energy is coupled, and hence several solutions for the perturbed value of β.

We assume that the perturbing medium is a liquid in which only longitudinal stress components can exist, and we take the substrate surface to be at $y = 0$. The presence of the liquid perturbs the boundary conditions at the substrate surfaces so that the normal component of stress at this surface is no longer zero. We assume the width of the acoustic beam to be w and the fields to be uniform in the x direction. In this case, Eq. (2.5.25) becomes

$$\frac{dA}{dz} + j\beta A = \frac{w}{4} v_{0y}^* \hat{T}_2 \tag{2.5.48}$$

where T_2 is the component of stress normal to the substrate and v_{0y} is the velocity normalized to unit power at the surface $y = 0$ of the unperturbed Rayleigh wave. The particle velocity in the y direction $\hat{v}_y$, associated with the Rayleigh wave, is defined as

$$\hat{v}_y = A v_{0y} \tag{2.5.49}$$

In this solution, we use the boundary condition on $\hat{v}_y$ but use Eq. (2.5.48) to account for the change in the boundary condition on T_2. We assume that the radiated wave has a particle velocity $\hat{v}$ in a direction θ to the substrate normal. The boundary conditions on continuity of v_y yield the relation

$$\hat{v} \cos \theta = A v_{0y} \tag{2.5.50}$$

The stress in a liquid is invariant with the angle. Thus

$$\hat{T}_2 = -Z_L \hat{v} = \frac{-Z_L A V_{0y}}{\cos \theta} \tag{2.5.51}$$

It follows from Eqs. (2.5.48)–(2.5.51) that

$$\frac{dA}{dz} + j\beta A = -\alpha A \tag{2.5.52}$$

where

$$\alpha = \frac{\omega v_{0y} v_{0y}^* Z_L}{4 \cos \theta} \tag{2.5.53}$$

The solution of Eq. (2.5.52) is

$$A(z) = A_0 e^{-(j\beta + \alpha)z} \tag{2.5.54}$$

where A_0 is the amplitude of the wave at $z = 0$. The value of v_{0y} can be found from the Rayleigh wave solution given in Sec. 2.3.4. This is the leaky wave we postulated.

After considerable algebra to evaluate the power flow per unit width of a surface acoustic wave, $P = -(w/2) \int (v_z T_3^* + v_y T_4^*)\, dy$, Auld [7] has shown that

$$v_{0y} v_{0y}^* = \frac{f_y \omega}{\rho_{m0} V_s^2 w} \tag{2.5.55}$$

where f_y is a dimensionless parameter of order unity, given by the relation

$$f_y = \left(\frac{V_s}{V_R}\right)^2 \frac{4\gamma^2[1 - (V_R/V_s)^2]^{3/2}}{3\gamma - 2\gamma(V_R/V_s)^2 - 1} \tag{2.5.56}$$

The parameters V_s and V_l are the shear and longitudinal phase velocities in the substrate, respectively, and

$$\gamma^2 = \frac{1 - (V_R/V_l]^2}{1 - (V_R/V_s)^2} \tag{2.5.57}$$

We often need the parameter f_y, as well as another useful parameter, f_z, which is defined by the relation

$$v_{0z} v_{0z}^* = \frac{f_z \omega}{\rho_{m0} V_s^2 w} \tag{2.5.58}$$

where

$$f_z = f_z/\gamma \tag{2.5.59}$$

Both these parameters, f_z an [illegible] as a function of V_s/V_l.

We can therefore write [illegible]m

$$\alpha = \frac{\omega f_y}{4\rho_{m0} V_s^2 \cos \theta} - \frac{Z_L}{4 Z_s} \frac{f_y}{\cos \theta} \tag{2.5.60}$$

where Z_s and k_s are the shear wave impedance and the propagation constant, respectively, in the substrate.

If $\alpha/\beta << 1$, the leaky wave attenuation due to radiation into a liquid is small when $Z_L << {}'_s$ (i.e., if the impedance of the liquid is low compared to the shear wave impedance of the substrate). Even air, for which $Z_L/Z_s << 1$, can cause attenuation; this effect is noticeable in very long SAW delay lines and at very high frequencies because α is linearly proportional to ω.

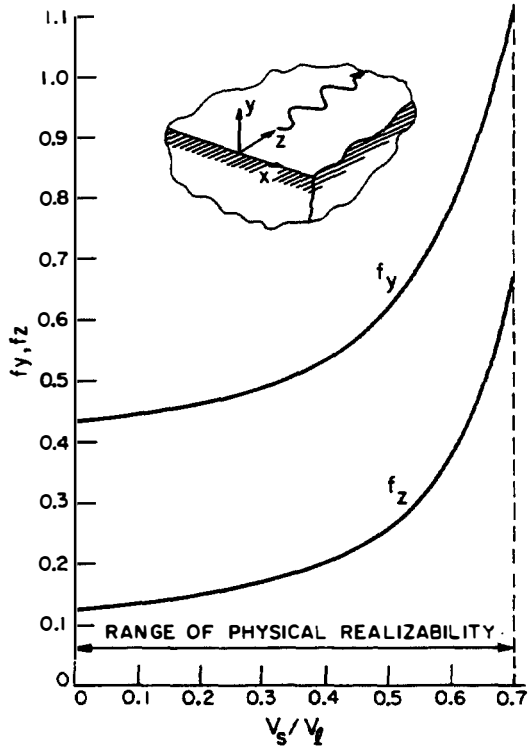

Figure 2.5.4 Field parameters f_y and f_z in Eqs. (2.5.56) and (2.6.58) as a function of the ratio of the bulk shear wave velocity V_s to the bulk longitudinal wave velocity V_l. (After Auld [7].)

This solution does not specifically depend on the fact that the substrate is isotropic. Provided that the parameter $v_{0y}v_{0y}^*$ can be calculated or measured for the substrate of interest, the leakage rate, or the attenuation α, can be determined from Eq. (2.5.53).

Example: Aluminum Substrate Loaded by Water

Consider an aluminum substrate with $V_s = 3.04$ km/s, $V_l = 6.42$ km/s, and $Z_s = 8.2 \times 10^6$ kg/m^2-s, on which a surface acoustic wave leaks into water with $Z_s = 1.5 \times 10^6$ kg/m^2-s and $V_L = 1.5$ km/s. We find that $Z_L/Z_s = 0.183$ and $V_s/V_l = 0.473$; thus Fig. 2.5.4 shows that $f_y = 0.58$ and Fig. 2.3.5 shows that $V_R/V_s = 0.94$ or $V_R = 2.86$ km/s. Hence $\theta = 31.6^0$ and $\alpha = 0.029k_R$ or $\alpha\gamma_R = 0.18$. The distance for the fields to drop to $1/e$ of their value at $z = 0$ is therefore 5.6 wavelengths.

2.5.6 Wedge Transducer

If power can radiate from the substrate, the reverse process can also occur, with a wave incident from the liquid exciting a surface acoustic wave on the substrate. Thus if a wave is incident on the substrate at the angle θ defined by Eq. (2.5.47), as shown in Fig. 2.5.5(a), we expect part of it to be reflected directly and the rest to excite a surface acoustic wave. Furthermore, as the surface acoustic wave propagates along the substrate, it will reradiate a wave at the angle θ [17–24].

On the other hand, if the region of excitation is kept short enough that there is little reradiation, the excitation length can be optimized to convert most of the incident energy into a surface acoustic wave. Thus a bulk or volume wave can be excited in water and, if incident at the correct angle on the substrate, will excite

a surface acoustic wave. Alternatively, a wedge-shaped solid material can be used, as shown in Fig. 2.5.5(b), to make an SAW transducer, known as a wedge transducer. These same principles are used to make prism couplers to optical waveguides [19].

We now consider a liquid wedge with the configuration shown in Fig. 2.5.5(b). We choose the incident longitudinal wave in the liquid medium to be at an angle θ to the normal, which excites Rayleigh waves cumulatively, as defined by Eq. (2.5.47). If the incident and reflected waves have particle velocities $\hat{v}_i$ and $\hat{v}_r$, respectively, the boundary conditions at the substrate are

$$(\hat{v}_i - \hat{v}_r)\cos\theta = -Av_{0y} \tag{2.5.61}$$

and

$$\hat{T}_2 = -Z_L(\hat{v}_i + \hat{v}_r) \tag{2.5.62}$$

where Z_L is the wave impedance of the wedge medium. Eliminating the reflected wave component $\hat{v}_r$ from Eqs. (2.5.61), (2.5.62), and (2.5.48) and assuming $T_4 = 0$ as before, we obtain the following differential equation for A:

$$\frac{dA}{dz} + j\beta A + \alpha A = -\frac{wZ_L\hat{v}_i v_{0y}^*}{2} \tag{2.5.63}$$

The parameter α corresponds to the leak rate or attenuation per unit length of the acoustic surface when the wedge material is present. From Eqs. (2.5.53) and (2.5.60), we find that

$$\alpha = \frac{wv_{0y}v_{0y}^*Z_L}{4\cos\theta} = \frac{Z_L}{Z_s\cos\theta}\frac{k_s f_y}{4} \tag{2.5.64}$$

We consider a wedge transducer of length $l\cos\theta$, which emits a parallel beam

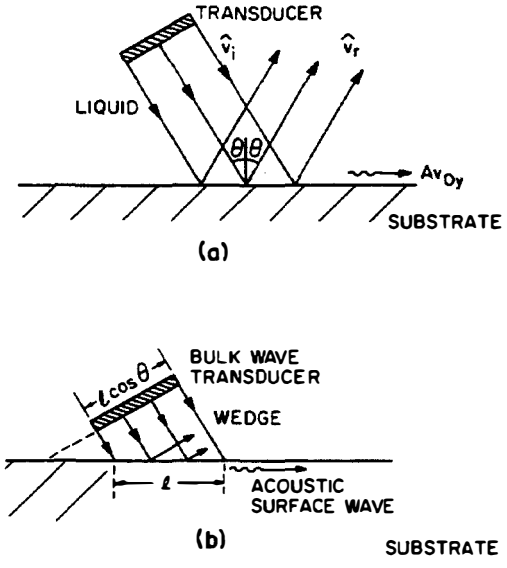

Figure 2.5.5 (a) Excitation of a surface wave from a liquid; (b) solid wedge transducer.

of length l in the z direction with a width w in the x direction. The total incident power on the substrate is

$$P_i(l) = \frac{1}{2} wl|v_i|^2 Z_L \cos\theta \tag{2.5.65}$$

To remove the phase factors, we write

$$A(z) = A_0(z)e^{-j\beta z} \tag{2.5.66}$$

and

$$\hat{v}_r(z) = V_r(z)e^{-j\beta z} = V_r(z)e^{-jk_L z\sin\theta} \tag{2.5.67}$$

It is also convenient to define the power density per unit length in the incident beam in terms of an amplitude A_i. From Eq. (2.5.65), for a length z,

$$P_i(z) = |A_i^2|z \tag{2.5.68}$$

where

$$\hat{v}_i(z) = A_i e^{-j\beta z} \frac{2}{wZ_L \cos\theta} = v_i e^{-j\beta z} \tag{2.5.69}$$

From Eqs. (2.5.65)–(2.5.69), Eq. (2.5.63) can be written in the form

$$\frac{dA_0}{dz} + \alpha A_0 = -A_i(2\alpha)^{1/2} \tag{2.5.70}$$

This equation can be integrated to determine $A_0(l)/A_i$. With the boundary condition $A_0(0) = 0$, the solution is

$$A_0(z) = -(1 - e^{-\alpha z}) A_i\left(\frac{2}{\alpha}\right)^{1/2} \tag{2.5.71}$$

The surface wave power excited by a transducer of length l is $|A_0(l)|^2$. Thus, from Eqs. (2.5.68) and (2.5.71), the conversion efficiency η is defined as

$$\eta = \frac{P_0(l)}{P_i(l)} = \frac{2(1 - e^{-\alpha l})^2}{\alpha l} \tag{2.5.72}$$

The efficiency is plotted as a function of αl in the upper curve ($\gamma/\alpha = 0$) of Fig. 2.5.6. It has a maximum value of 0.815 at $\alpha l = 1.26$ and half-power points at $\alpha l = 0.27$ and 4.8; thus the tolerance on the choice of the optimum value of αl is relatively loose. Since α is proportional to frequency, this is also a plot of efficiency versus frequency.

Finite attenuation. This excitation theory has also been modified to account for finite attenuation in the wedge. Due to the magnitude of the input velocity attenuation, the excitation at the substrate decays as $\exp(-\gamma z)$, while the

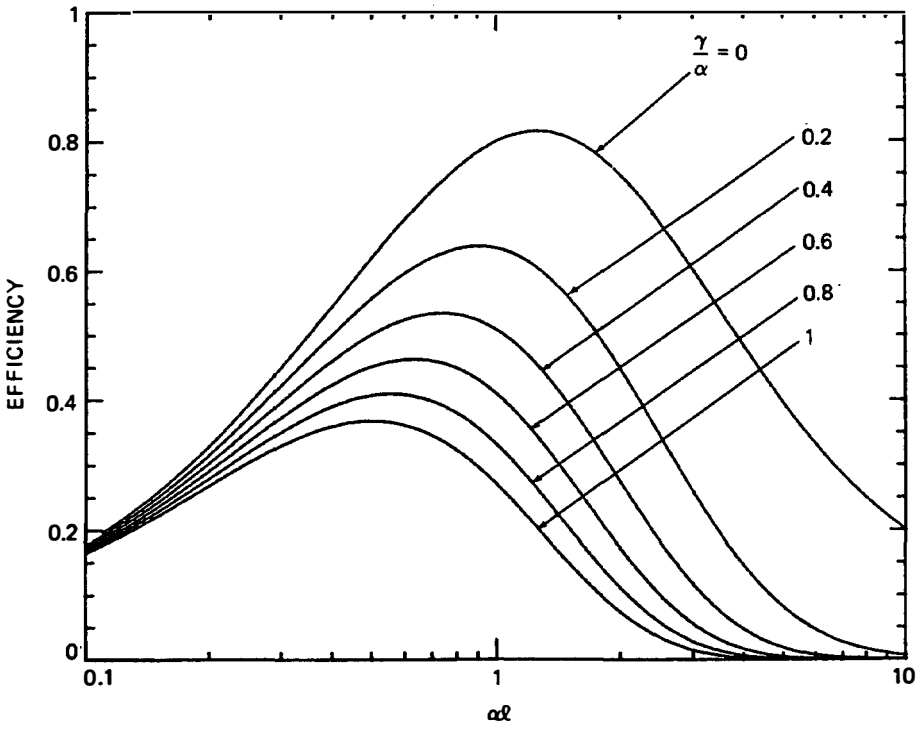

Figure 2.5.6 Wedge efficiency η versus normalized length or frequency αl for several values of wedge loss factor γ/α.

magnitude of the velocity at the transducer stays constant. The efficiency function η becomes

$$\eta = 2\alpha l e^{-2\gamma l}\left[\frac{1 - e^{-(\alpha-\gamma)l}}{(\alpha-\gamma)l}\right]^2 \tag{2.5.73}$$

Curves of η as a function of αl for different values of γ/α are plotted in Fig. 2.5.6.

Efficiency variation with incident angle or velocity. The variation of the efficiency can also be calculated as a function of the incident angle θ. If θ is not at its correct value θ_0, the incident wave will not excite a wave at the point z that is in phase with the wave traveling along the substrate that was excited at a point z'. Equation (2.5.72) can be modified to account for this effect and to solve the equations exactly. The physics of the problem lead us to expect that as the phase change in a length z is $\phi = k_L z \sin\theta$, the phase error $\Delta\phi$ due to a change in angle from the optimum value θ_0, where $k_L \sin\theta_0 = \beta$ to θ, is

$$\Delta\phi = (k_L \sin\theta - \beta)z \approx k_L z \cos\theta_0 \, \Delta\theta \tag{2.5.74}$$

where $\Delta\theta = \theta - \theta_0$. Thus, after a distance l, the phasor error $\Delta\phi$ is approximately

$$\Delta\phi \approx K\alpha l \tag{2.5.75}$$

where the velocity error is normalized and expressed by the parameter K as

$$K = \frac{k_L \sin \theta - \beta}{\alpha} \tag{2.5.76}$$

Beyond the point $\Delta\phi = \pi$, the induced signals will be out of phase with those induced earlier near $z = 0$. Thus when $\Delta\phi > \pi$, the efficiency will drop radically. Hence if $\alpha l \sim 1.3$, then $K < 4$ becomes the approximate condition for efficient power transfer.

A more complete treatment can be carried out by putting $\theta = \theta_0$ in Eqs. (2.5.61) and (2.5.62) but taking account of the phase change in the arguments of the exponentials. In this case, the efficiency is

$$\eta = \frac{2}{\alpha l} \frac{[e^{-\alpha l} - \cos(K\alpha l)]^2 + \sin^2(K\alpha l)}{1 + K^2} \tag{2.5.77}$$

This relation is plotted for different values of K in Fig. 2.5.7. These calculations show that, in agreement with the approximate physical arguments, the efficiency drops to half its synchronous value when $K \approx 3.5$. The optimum length for maximum energy transfer also decreases when the synchronous condition is not satisfied. If αl is kept at a value of 1.26, there is a 3-dB drop in output for $K \approx 2$. We observe that the 3-dB point occurs when the error in velocity along the substrate ΔV_R corresponds to

$$\frac{\Delta V_R}{V_R} = -\frac{\Delta\beta}{\beta} = \frac{K\alpha}{\beta} \tag{2.5.78}$$

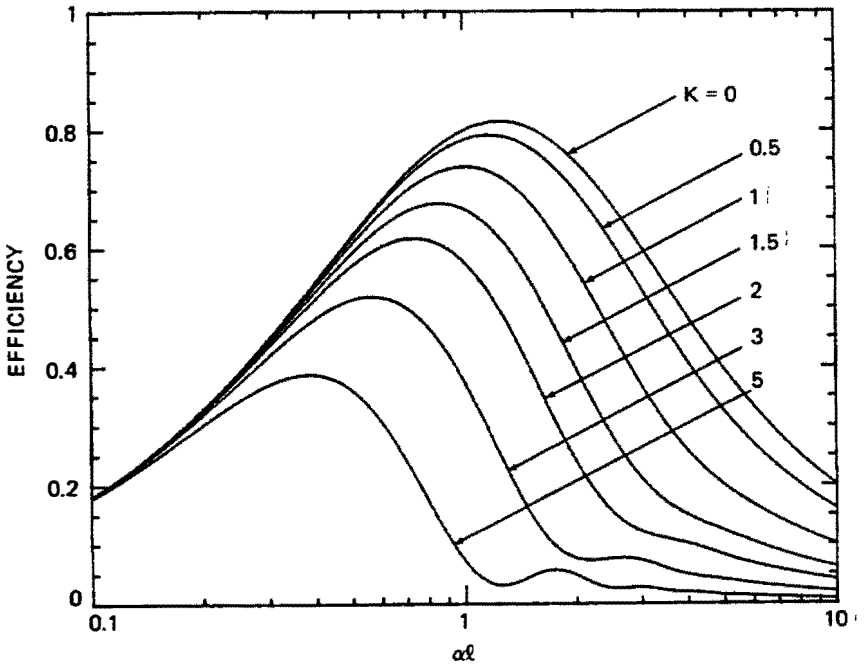

Figure 2.5.7 Plot of wedge transducer transduction efficiency versus αl for a different value of velocity mismatch parameter K, where $K = (k_L \sin \theta - \beta)/\alpha$.

Example: Excitation of Surface Acoustic Waves in Aluminum from Water

We can use the parameters already calculated in Sec. 2.5.5 for the example of leaky surface waves on aluminum in water. There we found that $\alpha = 0.18/\lambda_r$. Hence the optimum length l for transduction is 1.3/0.18, or 7.2 wavelengths. If we keep $\alpha l = 1.3$, then Fig. 2.5.7 indicates that for a K value of approximately 2, the efficiency drops by a factor of 3 dB. In turn, this implies an error in the incident angle corresponding approximately to $k_L \cos\theta\, \Delta\theta = K\alpha$ or $\Delta\theta = K\alpha\lambda_L/2\pi = K\alpha\lambda_R \sin\theta/2\pi$. This corresponds to an allowable error of $\pm 2°$ for a 3-dB drop in output or a velocity mismatch of $\pm 2\%$. The effect on the phase change of the reflected wave as the angle θ is varied may be considerably more critical, especially if $\alpha l >> 1$.

Reflected wave. Finally, we consider the wave reflected from the substrate. Assuming that $\theta = \theta_0$, it can be shown from Eqs. (2.5.61), (2.5.67), and (2.5.69) that, for the optimum angle of incidence,

$$V_r(z) = V_i(2e^{-\alpha z} - 1) \tag{2.5.79}$$

We observe that $V_r(z)$ is positive and equal to V_i at $z = 0$. At the point where $\alpha z = l\text{n}\, 2 = 0.69$, $V_r(z)$ becomes zero, reverses in sign, and increases to a magnitude V_i at large z. Thus, initially, there is a reflected beam; its amplitude then passes through zero and a second reflected beam generated by the leaky surface wave appears to be radiated from the region where $z > 0.69\alpha$. The radiated wave due to the surface acoustic wave excitation is π out of phase with the initial reflected wave and constant in amplitude for large z because the power lost is continually being made up by the excitation from the transducer.

The fact that the signal for large z suffers a π phase change is in marked contrast to the situation where no surface acoustic wave is excited. In this case there is no phase change. The implication is that if the transducer angle is changed by a small amount from the optimum, the surface acoustic wave excitation becomes weak and there is a π phase change in the reflected signal. Therefore, it is relatively easy to measure the proper angle for synchronism and, hence, the surface acoustic wave velocity of the substrate.

If the transducer excites the substrate only over a length l, the leaky wave will fall off in amplitude exponentially at points where $z >> l$.

Example: Reflection of Waves from Aluminum in Water

It follows from Eq. (2.5.79) that the reflected beam drops in amplitude by 3 dB from its initial value at the point where $z = 0.16/\alpha$. The amplitude becomes zero at $z = 0.69/\alpha$, changes phase, and rises to within 3 dB of its maximum value where $z = \Delta = 1.92/\alpha$. For excitation of Rayleigh waves on aluminum ($\alpha\lambda_r = 0.187$), we conclude that the specularly reflected beam has its first 3-dB point at $z = 0.16/0.18\lambda_r = 0.9\lambda_r$ or $z = 1.7\lambda_L$, while the zero point is at $z = 5.6\lambda_r$ or $z = 11\lambda_L$, respectively, and the 3-djB point of the shifted beam is at $D = 10.7\lambda_r$ or $D = 20\lambda_L$, respectively. This phenomenon was first predicted by Schock for Rayleigh waves, using a completely different method, and is known as the *Goos–Hänchen effect* in optics [20–23]. The initial theories predicted that there is a secondary beam emitted at a distance Δ along the substrate, whose value is very close to $1.92/\alpha$, as we have calculated [23].

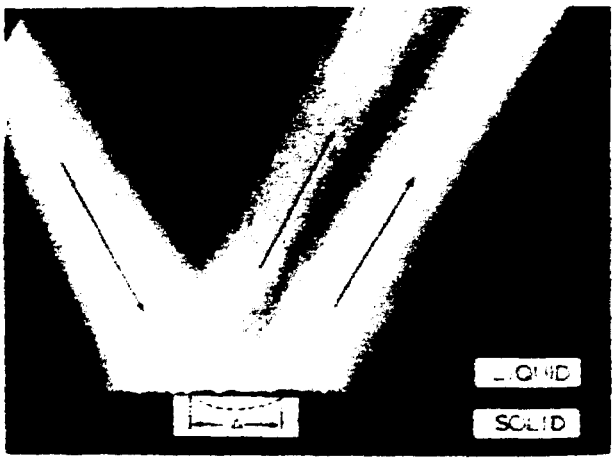

Figure 2.5.8 Schlieren photograph of an ultrasonic beam incident on a liquid–solid (aluminum) interface at the Rayleigh angle. The reflected beam, as indicated, is split into two components: a specularly reflected beam and a beam displaced a distance laterally down the interface. Secondary beams are visible at greater distances. (After Breazeale et al. [20].)

Experimental results. Wedge transducers have been made using a liquid medium and efficiencies up to 68% have been observed [24]. Thus for nondestructive testing or for SAW devices, it is obviously preferable to use a wedge of solid material and to excite and reradiate only over the optimum length l for which $\alpha l = 1.3$. The problem here is that the wedge transducer can generate both shear and longitudinal waves at the interface with the substrate, which lowers its efficiency. But choosing a wedge material that propagates only in a pure mode can circumvent this problem. One possibility is to use silicon rubber (RTV 615), which can propagate only longitudinal waves. At frequencies below 5 MHz, where this material is not too lossy, transducers with conversion efficiencies up to 35% have been constructed. At higher frequencies, polystyrene wedges have been employed to excite surface acoustic waves on ceramics with good efficiency; these are also often used on metals, because the coupling to the shear wave in the wedge is relatively weak and thus the shear wave is not strongly excited [24]. Several experiments have been carried out that clearly demonstrate the shift in the reflected beam excited by a beam of finite length. Excellent photos have been taken of this effect using Schlieren image techniques, as shown in Fig. 2.5.8.

Surface acoustic wave excitation from a liquid is important in materials testing because the change in amplitude of a surface acoustic wave as the angle of excitation by a bulk wave in water is varied, gives a very sensitive measure of the Rayleigh wave velocity. This basic phenomenon, discussed in Sec. 3.3.2, gives rise to the strong contrast effects of the scanned acoustic microscope, in which a lens in water is used to produce a highly convergent acoustic beam incident on a solid substrate. In turn, waves that are out of phase with the directly reflected waves are reradiated into the water. [25,26].

PROBLEM SET 2.5

1. **(a)** The power associated with the electric fields in a wave propagating through a piezoelectric material is

$$P_e = \tfrac{1}{2}\,\mathrm{Re}\int_s (\hat{\mathbf{E}} \times \hat{\mathbf{H}}^*) \cdot \mathbf{a}_z \, ds$$

Writing $\mathbf{E} \approx -\nabla\phi$ for a slow acoustic wave and using the vector relation

$$\nabla \times (\mathbf{A}\psi) = \psi\nabla \times \mathbf{A} + \mathbf{A} \times \nabla\psi$$

and Stoke's theorem, prove that

$$P_e = \tfrac{1}{2}\,\mathrm{Re} \int (j\omega \mathbf{D}\phi^*) \cdot \mathbf{a}_z\, ds$$

(b) Show that both the definitions of P_e above imply that $P_e = 0$ for a longitudinal plane acoustic wave traveling in the z direction through a piezoelectric medium poled in the z direction. Define $\mathbf{v}_0(x, y)$, $\mathbf{T}_0(x, y)$, $\phi_0(x, y)$, and $\mathbf{D}_0(x, y)$ for a forward wave.

2. A thin layer of water of thickness $h << \lambda$ is laid down on a surface wave substrate for which the Rayleigh wave velocity is V_r. Use the notation and parameters for a solid employed in Sec. 2.5 and take the density of the water to be ρ_w. Find the perturbed propagation constant of the surface wave when the substrate is mass loaded by the water layer.

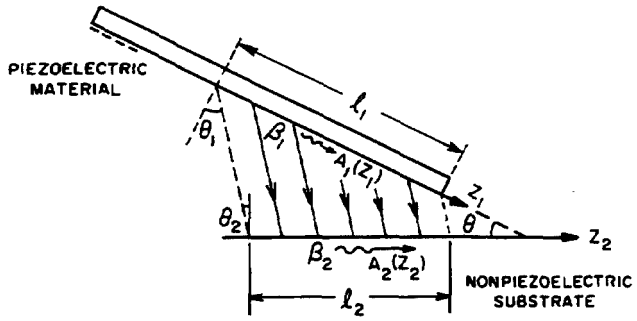

Note. The attenuation of the loaded surface wave will be zero. It is the real part of the propagation constant that is determined by the mass of the thin layer of water.

3. Acoustic waves can be excited in a conductor by electromagnetic $\mathbf{J} \times \mathbf{B}$ forces. Consider the electromagnetic acoustic transducer (EMAT) illustrated in the figure, which is used to excite Rayleigh waves. The magnet is used to excite a uniform β field parallel to the surface of the metal substrate. A meander line is placed very close to the substrate. A current I flows along the N elements of the transducer, which are spaced a distance $l/2 = \lambda/2$ apart, where λ is the Rayleigh wave wavelength. Assume that an identical current I is excited in the substrate just below each strip, and that the strips are each of length w and width l_1, spaced $l/2$ apart.

(a) By determining the total Rayleigh wave power excited, find the radiation resistance R_a (input resistance) of the meander line at the synchronous or center frequency, where $R_a = 2P_a/I^2$ and P_a is the acoustic power excited.

(b) Assume that the device is operated at a center frequency of 1 MHz, that $l_1 = l/4$, and that the wave is excited on aluminum. Suppose that the total resistance of the input circuit, including the meander line and surface resistance of the aluminum, is 1 Ω. Find the efficiency of excitation η by assuming that the inductance of the meander line is tuned out and the input is matched. In this case, the input power is $P_a = 1/2(R_a + R_0)I^2/2$, where R_a is the radiation resistance and R_0 is the resistance of the circuit (1 Ω). Thus the efficiency is

$$\eta = \frac{R_a}{2(R_a + R_0)}$$

where the factor of 2 compensates for the acoustic waves excited in each direction.

Note. The efficiency of this device is very low. Its advantage is that no contact has to be made between it and the substrate.

4. Consider the surface-to-surface (STS) wave transducer shown in the figure. A Rayleigh wave with a propagation constant $\beta_1 = \omega/V_{r1}$ is excited on a piezoelectric material. It radiates into water at an angle θ_1 to the normal. The piezoelectric substrate, which we will call substrate 1, is placed at an angle θ to a lower nonpiezoelectric substrate, which we will call substrate 2. The wave in the water between the two substrates excites a surface wave with a propagation constant $\beta_2 = \omega/V_{R2}$ on substrate 2. Determine the correct relations between the angles θ_1, θ_2, and θ, as shown in the figure, for optimum excitation. Assuming that the leak rates of waves from substrates 1 and 2 are α_1 and α_2, respectively, determine an expression for the power transferred in a length l_2 of the substrate 2. Consider the case for which $\alpha_1/\cos\theta_1 = \alpha_2/\cos\theta_2$ (you will need l'Hospital's rule). Find the optimum value of $\alpha_2 l_2$ for maximum power transfer and the corresponding theoretical maximum power transfer efficiency.

   Hint. It is convenient to use coordinates z_1 and z_2 for the top and bottom substrates, respectively. Remember that $A_1(0)$ is defined and that you must find $A_2(l_2)$ in terms of $Aj_1(0)$ and determine when $|A_2(l_2)/A_1(0)|^2$ is maximum.

5. Work out a similar analysis to that of Prob. 4 for two parallel substrates of the same material of equal velocity and interaction length l which are held parallel to each other. Assume that the separating medium is thick enough that the attenuation of the wave passing through it is η_0, and large enough that the radiated wave from the lower substrate has no influence on the upper substrate. Determine the optimum coupling value of αl for maximum power transfer and the maximum power transfer efficiency for this configuration. Ignore the loss η_0 in your definition of the leak rate α for the two substrates.

REFERENCES

1. L. D. Landau and E. M. Lifshitz, *Theory of Elasticity*, Vol. 7 of *Course of Theoretical Physics*, J. B. Sykes and W. H. Reid, trans. Oxford: Pergamon Press Ltd., 1959.
2. Y. C. Fung, *Foundations of Solid Mechanics*. Englewood Cliffs, N.J.: Prentice-Hall, Inc., 1965.
3. W. M. Ewing, W. S. Jardetsky, and F. Press, *Elastic Waves in Layered Media*. New York: McGraw-Hill Book Company, 1957.
4. B. A. Auld, *Acoustic Fields and Waves in Solids*, Vol. I. New York: John Wiley & Sons, Inc., 1973.
5. J. F. Nye, *Physical Properties of Crystals: Their Representation by Tensors and Matrices*, corr. rpt. of 1st ed. (1957: rpt. Oxford: Clarendon Press, 1960).
6. R. C. McMaster, ed., *Nondestructive Testing Handbook*, 2 vols. New York: Roland Press, 1959.
7. B. A. Auld, *Acoustic Fields and Waves in Solids*, Vol. II. New York: John Wiley & Sons, Inc., 1973.
8. Lord Rayleigh, "On Waves Propagated Along the Plane Surfaces of an Elastic Solid," *Proc. London Math. Soc.*, 17 (1885), 4–11.
9. B. A. Auld and G. S. Kino, "Normal Mode Theory for Acoustic Waves and Its Application to the Interdigital Transducer," *IEEE Trans. Electron Devices*, ED-18, No. 10 (Oct. 1971), 898–908.

10. I. A. Viktorov, *Rayleigh and Lamb Waves: Physical Theory and Applications.* New York: Plenum Press, 1967.
11. W. R. Smith, H. M. Gerard, J. H. Collins, T. M. Reeder, and H. J. Shaw, "Analysis of Interdigital Surface Wave Transducers by Use of an Equivalent Circuit Model," *IEEE Trans. Microwave Theory Tech.*, MTT-17, No. 11 (Nov. 1969), 856–64.
12. K. A. Ingebrigtsen, "Surface Waves in Piezoelectrics," *J. Appl. Phys.*, 40, No. 7 (June 1969), 2681–86.
13. A. K. Ganguly and M. O. Vassell, "Frequency Response of Acoustic Surface Wave Filters," *J. Appl. Phys.*, 44, No. 3 (Mar. 1973), 1072–85.
14. G. S. Kino and J. Shaw, "Acoustic Surface Waves," *Sci. Am.*, 227, No. 4 (Oct. 1972), 50–68.
15. S. Ramo, J. R. Whinnery, and T. Van Duzer, *Fields and Waves in Communication Electronics.* New York: John Wiley & Sons, Inc., 1965.
16. R. N. Bracewell, *The Fourier Transform and Its Applications*, 2nd ed. New York: McGraw-Hill Book Company, 1978.
17. W. G. Neubauer, "Ultrasonic Reflection of a Bounded Beam at Rayleigh and Critical Angles for a Plane Liquid-Solid Interface," *J. Appl. Phys.*, 44, No. 1 (Jan. 1973), 48–55.
18. H. L. Bertoni and T. Tamir, "Characteristics of Wedge Transducers for Acoustic Surface Waves," *IEEE Trans. Sonics Ultrason.*, SU-22, No. 6 (Nov. 1975), 415–20.
19. P. K. Tien and R. Ulrich, "Theory of Prism-Film Coupler and Thin-Film Light Guides," *J. Opt. Soc. Am.*, 60, No. 10 (Oct. 1970), 1325–37.
20. M. A. Breazeale, L. Adler, and G. W. Scott, "Interaction of Ultrasonic Waves Incident at the Rayleigh Angle onto a Liquid-Solid Interface," *J. Appl. Phys.*, 48, No. 2 (Feb. 1977), 530–37.
21. A. Schoch, "Seitliche Versetzung eines total reflektierten Strahls bei Ultraschallwellen," *Acustica*, 2, No. 1 (1952), 18–19.
22. F. Goos and H. Hänchen, "Ein neuer und fundamentaler Versuch zur Totalreflexion," *Ann. Phys.* (Leipzig), 1, No. 6 (1947), 333–46.
23. L. M. Brekhovskikh, *Waves in Layered Media*, R. T. Beyer, trans., 2nd ed. New York: Academic Press, Inc., 1980.
24. J. Fraser, B. T. Khuri-Yakub, and G. S. Kino, "The Design of Efficient Broadband Wedge Transducers," *Appl. Phys. Lett.*, 32, No. 11 (June 1978), 698–700.
25. R. D. Weglein, "Metrology and Imaging in the Acoustic Microscope," in *Scanned Image Microscopy*, E. A. Ash, ed. London: Academic Press, Inc. (London) Ltd., 1980, pp. 127–36.
26. C. F. Quate, "Microwaves, Acoustics and Scanning Microscopy," in *Scanned Image Microscopy*, E. A. Ash, ed. London: Academic Press, Inc. (London) Ltd., 1980, pp. 23–55.
27. H. Engan, "Excitation of Elastic Surface Waves by Spatial Harmonics of Interdigital Transducers," *IEEE Trans. Electron Devices*, ED-16, No. 12 (Dec. 1969), 1014–17.